The Effective Temperatures of Hot Stars II. The Early-O Types. [1]

Miriam Garcia[1] and Luciana Bianchi

Center for Astrophysical Sciences
The Johns Hopkins University, Dept. of Physics and Astronomy
3400 N. Charles St., Baltimore, MD 21218, USA.

garcia@pha.jhu.edu, bianchi@pha.jhu.edu

ABSTRACT

We derived the stellar parameters of a sample of Galactic early-O type stars by analysing their UV and Far-UV spectra from *FUSE* (905-1187Å), *IUE*, *HST-STIS* and *ORFEUS* (1200-2000Å). The data have been modeled with spherical, hydrodynamic, line-blanketed, non-LTE synthetic spectra computed with the *WM-basic* code. We obtain effective temperatures ranging from $T_{\rm eff}$= 41,000 K to 39,000 K for the O3-O4 dwarf stars, and $T_{\rm eff}$= 37,500 K for the only supergiant of the sample (O4 If^{+}). Our values are lower than those from previous empirical calibrations for early-O types by up to 20%. The derived luminosities of the dwarf stars are also lower by 6 to 12%; however, the luminosity of the supergiant is in agreement with previous calibrations within the error bars. Our results extend the trend found for later-O types in a previous work by Bianchi & Garcia.

Subject headings: Stars: fundamental parameters — stars: mass loss — stars: early-type — stars: winds, outflows — ultraviolet: stars

---

[1]Departamento de Astrofísica, Universidad de La Laguna, Avda. Astrofísico Francisco Sánchez s/n, 38206 La Laguna (Tenerife), Spain.

[1]Based on observations with the NASA-CNES-CSA *Far Ultraviolet Spectroscopic Explorer (FUSE)* , which is operated by The Johns Hopkins University under NASA contract NAS5-32985, on *International Ultraviolet Explorer* (*IUE*) observations from the MAST and INES archives and on MAST archival data from the *Hubble Space Telescope* (*HST*) and the *Orbiting Retrievable Far and Extreme Ultraviolet Spectrometers* (*ORFEUS*) mission.

1. INTRODUCTION

Hot massive stars have a great impact on the surrounding interstellar medium (*ISM*) and play a crucial role in the chemical evolution of galaxies. Their strong ultraviolet radiation is responsible for the ionization of nearby *HII* regions where their stellar winds blow vast bubbles. Their supersonic wind outflows and the supernova explosion at the end of their evolution transfer energy and momentum to the *ISM* and disperse the material processed in the stellar interiors, thus setting the conditions for the formation of subsequent generations of stars.

The determination of the physical parameters of massive stars is therefore of great interest, yet complicated. High resolution spectroscopy is needed. Modeling the stellar atmosphere requires to account for the expanding wind, the non local thermodynamic equilibrium (non-LTE) conditions and the so called line-blanketing that modifies the flux distribution, especially at short wavelengths.

Spectroscopy in the ultraviolet and far ultraviolet ranges (hereafter UV and Far-UV) is a powerful tool to study the winds of massive stars since these spectral regions contain the resonance lines of the most abundant ions in the wind. In this work we analyse spectra from the *Far Ultraviolet Spectroscopic Explorer* (*FUSE*) (Moos et al. 2000), covering the 905-1187Å region, in conjunction with spectra at longer wavelengths (1200-2000Å) from the *International Ultraviolet Explorer* (*IUE*), the *Orbiting Retrievable Far and Extreme Ultraviolet Spectrometers* (*ORFEUS*) and the *Space Telescope Imaging Spectrograph* (*STIS*) aboard the *Hubble Space Telescope* (*HST*). The *FUSE* spectra allows us to uniquely constrain the stellar parameters by adding new ionization stages to those accessible to *IUE*, *ORFEUS* and *HST-STIS* (e.g. Bianchi et al. (2000), Bianchi & Garcia (2002)).

This is the second paper of a series devoted to provide accurate and consistent determination of the stellar parameters of Galactic massive stars with this method. Bianchi & Garcia (2002, hereafter paper I) studied six mid-O type stars and found effective temperatures lower (by 15-20%) than previously determined for the sample stars or calibrated for their spectral types. In this work we perform a similar analysis for early-O type stars. The paper is organized as follows. In Section 2 we provide details about the data and the reduction. In Section 3 we summarize the relevant information from the literature about the program stars. In Section 4 we compare the spectral line characteristics. The stellar parameters are derived in Section 5 by modeling the spectra. In Section 6 the results are discussed.

2. DATA AND REDUCTION

For all the program stars we analysed *FUSE* spectra (905-1187Å) and UV archival spectra ($\lambda > 1200$Å) from *IUE*. For a few objects we also used *ORFEUS* and *HST-STIS* archival data. The datasets used are listed in Table 1.

The *FUSE* data, taken through the *LWRS* aperture ($30'' \times 30''$), have a resolution of $\lambda/\Delta\lambda \geq 20{,}000$. The data were processed with the pipeline (CalFUSE) version 2.0.5 (Dixon, Kruk, & Murphy 2001). All the LiF and SiC segments were examined to assure optimal centering of the spectra in the extraction window and to avoid data defects such as event bursts or the "worm" (Sahnow et al. 2000; Sahnow 2002). The good portions from different channels were combined, after the consistency of wavelength scale and flux level was checked, to achieve the maximum S/N. The wavelength ranges 905-930Å and 1181-1187Å, at the ends of the *FUSE* range, have poor spectral quality and were not used in this work. The data in the 1082.5-1087Å region come entirely from the SiC channels, therefore the He II λ1084.9 line was given a small weight in the analysis. The resulting combined spectra, normalized to the local continuum, are shown in Figure 1.

The *FUSE* wavelength range contains several absorption lines and bands of interstellar atomic and molecular hydrogen. In order to assess which features in the spectrum are purely stellar and to determine reliable continuum points for flux normalization, we calculated the $H_2 + HI$ absorption spectrum for the line of sight of each star. We used measurements of hydrogen column densities when available in the literature or, otherwise, we estimated the column densitiy from color excesses using the relations from Bohlin, Savage, & Drake (1978): $N_H/E(B-V) = 5.8 \cdot 10^{21}\ atoms\ cm^{-2}mag^{-1}$, where $N_H = N_{HI} + 2N_{H_2}$, and $N_{HI}/E(B-V) = 4.8 \cdot 10^{21}\ atoms\ cm^{-2}mag^{-1}$. The hydrogen ($HI + H_2$) absorption models are plotted over the observed spectra in Figures 1, 3, 5 and 7.

We examined all the existing *IUE* observations of the program objects taken with the SWP camera (1150-1975Å), using the on-line tools of the MAST archive, to check for variability and to exclude saturated portions, and chose the data with the best S/N. High dispersion *IUE* spectra ($\Delta\lambda \approx 0.2$Å) are available for all objects except for HD 64568, for which only a low dispersion spectrum ($\Delta\lambda \approx 6$Å) exists. We then downloaded the selected spectra from the INES archive (Wamsteker et al. 2000) because the data typically have a better background correction at wavelengths shorter than 1400Å than the data in the MAST archive. We additionally used *HST-STIS* spectra ($0.2''$x$0.09''$ aperture and E140H grating, 1150-1700Å, $\lambda/\Delta\lambda$=114,000) for two objects and *ORFEUS-TUES* spectra (900-1400Å, $\lambda/\Delta\lambda$=10,000) for one program object. These data were downloaded from the MAST archive. The normalized spectra in the UV range that contains the strongest spectral lines (1200-1750Å) are shown in Figure 2.

3. THE PROGRAM STARS

We performed an exhaustive literature search about the program stars and collected all data useful to this study. In particular, we searched for reliable spectral classifications and information about multiplicity and the environment of the stars. Table 2 compiles the spectral classification and other relevant data, including the hydrogen column densities in the line of sight of each object. A discussion on the individual objects is given in the following section.

3.1. HD 190429A

HD 190429 is a multiple system that belongs to the Cygnus OB3 association. HD 190429A has three companions (B,C,D) located at 1.7″, 42.5″ and 29.0″ respectively (Abt 1986), therefore only the B component is included in the *FUSE* and *IUE* large apertures. The D component may be at the edge of the *FUSE LWRS* slit, but it is considerably fainter than HD 190429A (Δ V $\sim$ 4, Abt (1986)). Mason et al. (1998) reports a companion of HD 190429A at a 0.09″ distance, but we found no further information on this object.

For HD 190429A we adopt a spectral type of O4 If$^+$ (Walborn 1972, 1973) and O9.5 II for the B component (Walborn & Howarth 2000). The luminosity class of the secondary varies in the literature from Ibp (Morgan et al. 1955), to III (Abt 1986; Conti & Leep 1974; Guetter 1968). In Section 5.2 we estimate that its contribution to the total flux amounts to 15% at most. We examined the sixteen large aperture high resolution *IUE* spectra of HD 190429A taken with the SWP camera. Since we found no significant variation in the flux levels and the line profiles, we include this object in our analysis. The study of HD 190429A is of particular interest, because it is the only supergiant star earlier than O5 observed with *FUSE* except for HD 93129A (O2If*), which also belongs to a binary system.

The *IUE* spectrum of HD 190429A shows characteristics intermediate between O3 If* and O5 If$^+$ in the UV morphological sequence described by Walborn & Nichols-Bohlin (1987). Conti et al. (1995) concur that the UV spectral morphology of HD 190429A is typical of an O4-O5 If$^+$ star, but found that its IR spectrum (K-band) resembles that of a Wolf-Rayet, indicating the presence of a strong wind. Morris, Eenens and Blum (1996) obtained similar results. Walborn & Howarth (2000) found that the emission of Hα and He II λ4686 in HD 190429A is stronger than in other O3-O5 If$^+$ stars, again suggesting that HD 190429A is evolving to the WN stage. However, the mass-loss rate we derive (Section 5) is consistent with that predicted by the radiation pressure driven wind theory (Section 6).

3.2. HD 64568

HD 64568 belongs to NGC 2467/Puppis OB2 (Havlen 1972) and is one of the ionizing stars of the irregular *HII* region Sh 2-311 (Sharpless 1959). HD 64568 is a primary standard for the O3 V((f*)) type in the recent revision of the spectral classification of early type objects by Walborn et al. (2002a), based on optical spectra. We adopt this spectral classification, although other works are discrepant: MacConnel & Bidelman (1976), Crampton (1971), Cruz-Gonzalez et al. (1974) and Lodén (1965) classify HD 64568 as O5; Houk & Smith-Moore (1988) as O5/6 . None of these works provided luminosity class. Garrison et al. (1977) classified the star as O4 V ((f)) and Peton-Jonas (1981) as O5 V. The UV and Far-UV spectral morphology is consistent with the O3 V((f*)) classification.

We did not find conclusive reports about binarity. Solievella & Niemela (1986) analysed medium dispersion CTIO spectra and found radial velocity variations, but could not determine whether they are due to binarity or to instabilities in the atmosphere. Crampton (1972) obtained several measurements of the radial velocity, and found a maximum variation of 10 km s^{-1}.

3.3. HD 93250

HD 93250 is located in the Carina Nebula (NGC 3372), an *HII* region consisting of four lobes ionized by several stellar clusters, including Trumpler 14 and Trumpler 16 (Tr 14 and Tr 16). HD 93250 belongs to Tr 16. We adopt the spectral type O3.5 V((f^+)) from Walborn et al. (2002a). Other authors agree that HD 93250 is a dwarf star (O3 V((f)) (Walborn 1982, 1971a), O3:V((f)) (Levato & Malaroda 1982) and O3 V(f) (Thackeray & Andrews 1974)). However, HD 93250 is one of the brightest stars in the Carina complex (V = 7.37, Feinstein (1982)). Conti & Frost (1977) found evidence of a luminosity class higher than V and classified the star as O3 (providing no luminosity class). According to Mathys (1988), the star is a giant (O3 III(f)) and Penny et al. (1996) classified it as a supergiant (O3 I) based on its UV spectrum. We find that the FUSE spectrum (see Figure 1) does not display the characteristic signatures of supergiants, i.e. the S IV $\lambda\lambda$1062.7,1073.0,1073.5 and P V $\lambda\lambda$1118.0,1128.0 P Cygni profiles (see paper I and Figures 1 and 3 of this paper), supporting the luminosity class V. On the other hand, the radius we derive from line fitting (see Secton 5.1.2) is larger than for the other O3.5 V((f^+)) star of the sample, consistently with the higher luminosity of HD 93250.

Walborn & Panek (1984) studied the UV-morphology of the early type dwarf stars and found no anomaly in the *IUE* spectrum of HD 93250, except for the unsaturated profile

of C IV λλ1548.2,1550.8. They suggested that an unresolved later-type companion could be a possible explanation. Levato et al. (1991) measured a constant heliocentric radial velociy and concluded that the star is not a binary; no companion was found in the speckle interferometric survey of Mason et al. (1998). We will further discuss this point in Section 5.1.2.

3.4. HD 93205

HD 93205 is part of a multiple system, again located in the Tr 16 cluster. HD 93205 is a spectroscopic binary with additionally a visual companion (HD 93204, O5 V) at a 18.7″ distance (Mason et al. 1998), which may be included in the *FUSE LWRS* aperture, but not in the *IUE* large aperture. The primary component of the HD 93205 system is consistently classified in the literature as O3 V (see Table 2) but revised to O3.5 V((f$^+$)) by Walborn et al. (2002a), which we adopt. Conti & Walborn (1976) and Morrell et al. (2001) provided spectral classification for both components of the system: O3 V+O8 V.

The question whether HD 93205 is an eclipsing binary is not settled. From the inclination angle (i $\simeq$ 45°-53°, Conti & Walborn (1976)) no eclipses are expected. Antokhina et al. (2000) found photometric variability in the system of a maximum of $\sim 0^m.02$, which they explained with a non uniform brightness distribution. The latest photometric study (van Genderen 2003) suggests instead that the light curve variations (amplitude $0^m.02$) are due to eclipses. The only large aperture *IUE* spectra, SWP14747 and SWP07959, were taken at phases Φ=0.78 and Φ=0.28 (calculated using the orbital parameters from Stickland & Lloyd (1993)); the orbital positions of the secondary at these phases are equivalent for the observer and, in fact, the spectrum does not vary.

The FUSE and IUE spectra of HD 93205 look very similar to those of HDE 303308 (which has a similar spectral type) and the wind lines clearly originate from the O3.5 V((f$^+$)) star, while the secondary component (O8 V) may contribute to the continuum. The spectral analysis shows that this contribution is of the order of $< 15\%$ (see Section 5.1.1).

3.5. HDE 303308

HDE 303308, located 1′ North of η Carinae, also belongs to the Tr 16 cluster in the Carina Nebula. We adopt the spectral classification of Walborn et al. (2002a), O4 V((f$^+$)), although the star has been previously classified as O3 dwarf (see Table 2). Speckle interferometry indicates that HDE 303308 is a single star (Mason et al. 1998). Levato et al.

(1991) report variability of the radial velocity, but could not determine whether the star belongs to a binary system. Stickland & Lloyd (2001) measured the radial velocity from three IUE spectra and found no significant changes. van Genderen et al. (1989) did not find any photometric variations.

3.6. HD 96715

HD 96715 belongs to the Carinae OB2 association, rich in luminous massive stars. The spectral classifications throughout the literature are in general agreement. We adopt O4 V((f)) (Walborn 1973; Cruz-Gonzalez et al. 1974); other similar classifications are listed in Table 2. HD 96715 is a blue straggler and displays an unusually strong N III λ4514 line for its early type that may indicate nitrogen enrichment (Schild & Berthet 1986). There are no studies on binarity.

For this star we use a combination of two large aperture *IUE* spectra out of eight available in the archive. We use SWP43980 for $\lambda < 1700$Å, which has the best S/N ratio in this spectral region, but it is saturated for $\lambda > 1700$Å where we use SWP21999.

3.7. HD 168076

HD 168076 is a member of the young open cluster NGC 6611 (Walker 1961), located near the outermost part of the Sagittarius-Carina spiral arm. The spectral classification we adopt is O4 V((f)) (Walborn 1973). Other authors provide similar classifications (see Table 2) except for Mathys (1988): O4 III(f) and Hillenbrand et al. (1993): O5 V((f*)). Rachford et al. (2002) studied the line of sight of HD 168076 from its *FUSE* spectra and calculated the column densities of HI and H_2 (listed in Table 2) which we use in this analysis.

HD 168076 is a visual binary. Duchêne et al. (2001) resolved the components with a high angular resolution (0.035″) adaptive optics system and estimated a separation of $\sim$ 0.15″ and a difference in magnitude of ΔK=1.57. However, the line spectrum of HD 168076, very similar to the spectra of the other O4 dwarf stars in the sample, is apparently dominated in the Far-UV and UV ranges by the lines from the hot component.

There is only one high dispersion *IUE* spectrum of this object. It has some saturated portions, removed from the plots in Figures 2 and 6 and not considered in the analysis.

4. ANALYSIS OF THE SPECTRAL MORPHOLOGY

Examination of the UV and Far-UV spectra of the sample stars reveals the correspondence of the line morphology in this spectral region with the spectral classifications derived from the optical range. The general behaviour of the spectral lines as a function of spectral type and luminosity class has been described in a number of atlases, both in the *IUE* range (Walborn, Nichols-Bohlin, & Panek 1985) and in the *FUSE* range (Pellerin et al. (2002) for Galactic stars, Walborn et al. (2002b) for Magellanic Cloud stars). In this section we provide a more detailed discussion of the spectral morphology within the spectral types covered in this work and paper I. In the quantitative spectral modeling (Section 5) the observed line variations will be explained in terms of physical parameters.

4.1. Luminosity Effects at O4

The *FUSE* and *IUE* spectra of the O4 type stars are shown in Figures 1 and 2. The sample consists of one supergiant star (HD 190429A) and three dwarf stars (HDE 303308, HD 96715 and HD 168076). The *FUSE* satellite has not observed any giant star of type O4 (or earlier) yet.

The most prominent variations among luminosity classes are the different strength of P V $\lambda\lambda$1118.0,1128.0 in the *FUSE* range and Si IV $\lambda\lambda$1393.8,1402.8, He II λ1640 and N IV $\lambda\lambda$1718.0,1718.5 in the *IUE* range. P V $\lambda\lambda$1118.0,1128.0, Si IV $\lambda\lambda$1393.8,1402.8 and He II λ1640 display wind profiles in the spectrum of the supergiant star but are photospheric absorptions in the dwarf stars. S IV $\lambda\lambda$1062.7,1073.0,1073.5, which shows a P Cygni profile in HD 190429A (though severely masked by interstellar hydrogen absorption), and C IV λ1169+C IIIλ1176 change similarly. The behaviour of these lines is similar to what we found for mid-O types (paper I) and it is caused by the mass-loss rate variation with luminosity. In the present sample, the S IV $\lambda\lambda$1062.7,1073.0,1073.5 and C IV λ1169+C IIIλ1176 profile changes are not as remarkable as in later types because these lines are much less conspicuous due to the higher $T_{\rm eff}$.

Note that O VI $\lambda\lambda$1031.9,1037.6 displays a well developed P Cygni profile of similar strength at all luminosity classes as already seen in mid-O type stars (paper I). Similarly, the lines of other high ionization species, N V $\lambda\lambda$1238.8,1242.8 and C IV $\lambda\lambda$1548.2,1550.8, do not vary appreciably because they are saturated.

4.2. Temperature Effects

We find systematic line variations when we compare the spectra of the O3-O4 type stars analysed in this paper to the later type stars from paper I. Despite their many similarities, the spectra of O3-O6 dwarf stars in Figures 1 and 2 display clear $T_{\rm eff}$ effects. Notably, C IV λ1169+C IIIλ1176 and P V $\lambda\lambda$1118.0,1128.0+Si IV $\lambda\lambda$1122.5,1128.3,1128.4 decrease towards earlier types. In the *IUE* range, the weaker Si IV $\lambda\lambda$1393.8,1402.8 and stronger N IV $\lambda\lambda$1718.0,1718.5, O V λ1371.0 and C IV $\lambda\lambda$1548.2,1550.8 also indicate higher $T_{\rm eff}$.

The line variations with spectral type are more remarkable in the supergiants, as wind features are more developed in their spectra. When we compare the *FUSE* spectra of O4 and O6.5 supergiants (see Figure 3) we find the latter to have stronger S IV $\lambda\lambda$1062.7,1073.0,1073.5 and C IV λ1169+C IIIλ1176, whereas O VI $\lambda\lambda$1031.9,1037.6 does not vary. P V $\lambda\lambda$1118.0,1128.0 has a P Cygni profile in both stars, however with different shapes, indicating a different ionization structure in the wind.

In the *IUE* range (see Figure 4), the lines showing the largest variation are Si IV $\lambda\lambda$1393.8,1402.8 and He II λ1640. The strength of Si IV $\lambda\lambda$1393.8,1402.8 drastically decreases from HD 163758, where it is a fully developed P Cygni profile, to HD 190429A. The spectrum of HD 190429A displays a strong emission of He II λ1640.0, characteristic of O3-O5 If stars (Walborn, Nichols-Bohlin, & Panek 1985; Walborn & Nichols-Bohlin 1987). N IV $\lambda\lambda$1718.0,1718.5 and the emission of C IV$\lambda\lambda$1548.2,1550.8 increase from type O6.5 to O4. The strength of the feature at 1500Å, which we believe to be a S V line possibly contaminated with Si III lines (see paper I), is approximately the same in both spectra. The absorption line of O V λ1371.0 is present only in the spectra of the hotter star, HD 190429A.

5. QUANTITATIVE SPECTRAL MODELING

In this section we determine the photospheric and wind parameters of the sample stars by fitting their Far-UV and UV spectra with spherical, hydrodynamic, line-blanketed, non-LTE synthetic models. The models were calculated with the version 2.11 of the *WM-basic* code (Pauldrach, Hoffmann, & Lennon 2001), but have the 'solar' abundances of the previous version (*WM-basic* 1.22) for consistency with the grid of models constructed for paper I.

Our study takes into account the effects of shocks in the wind. Shocks produce soft-X rays in the expanding atmosphere which affect the ionization of several species, most remarkably O VI and N V. By modeling the lines of highly ionized atoms in the *FUSE* and *IUE* ranges consistently with the other spectral features, we can determine the value of the parameter $L_{\rm x}/L_{\rm bol}$, and thus provide a unique solution for the stellar parameters ($T_{\rm eff}$,

log g , R_*, v_∞ and $\dot{M}$).

We have built a vast grid of *WM-basic* models which -by comparison to the observed spectra- provides upper and lower limits of the stellar parameters. The final values and their uncertainties are obtained by computing models that refine the grid within the range of interest for each observed spectrum. In the following section we provide further details of the fitting process. The best fit models are shown in Figures 5-7. The derived stellar parameters are compiled in Table 3.

5.1. The Dwarf Stars

The spectra of the dwarf stars are mostly similar, except for subtle line variations (see Section 4.2). Therefore we follow a similar procedure to fit their spectra, which we explain in this section. The analysis of HD 93250 and HD 64568 is slightly different and the details are given in Sections 5.1.2 and 5.1.3.

We learned from our grid of models that P V $\lambda\lambda$1118.0,1128.0, C IV λ1169+C III λ1176, O V λ1371.0 and N IV $\lambda\lambda$1718.0,1718.5 are good temperature indicators in the interval of $T_{\rm eff}$ of 38,000 K to 42,000 K (enclosing the temperatures of our sample as we will see) and mass-loss rates of 10^{-7} to 10^{-6} $M_\odot$ yr^{-1}; we initially assumed log g = 4 and R_*= $9R_\odot$, adequate for luminosity class V. In this range of parameters, P V $\lambda\lambda$1118.0,1128.0 and C IV λ1169+C III λ1176 decrease with temperature; both lines are photospheric and therefore insensitive to changes of $\dot{M}$ and $L_{\rm x}/L_{\rm bol}$. The strength of N IV $\lambda\lambda$1718.0,1718.5 increases with $T_{\rm eff}$ and $\dot{M}$ and marginally decreases with higher $L_{\rm x}/L_{\rm bol}$. O V λ1371.0 has a hard threshold, and forms only in models with $T_{\rm eff}\geq$ 40,000 K (independently of shocks and mass-loss rate) thus providing an upper limit to the temperature of stars not displaying this line. When O V λ1371.0 is present in the stellar spectrum, its strength varies similarly to N IV $\lambda\lambda$1718.0,1718.5 and helps us constrain $L_{\rm x}/L_{\rm bol}$ and $\dot{M}$.

We can set solid limits to the interval of possible temperatures of the dwarf stars, based on the strength of these lines in their spectra. HD 64568, HD 93250, HD 93205 and HDE 303308 must have a temperature higher or equal than 40,000 K since their spectra display the O V λ1371.0 line. For these stars, the upper limit to $T_{\rm eff}$ is 42,000 K, because at higher temperatures (in the range of $\dot{M}$ set above), O V λ1371.0 becomes a fully developed P Cygni profile in the models, not seen in any stellar spectra, and N IV $\lambda\lambda$1718.0,1718.5 is not as strong as observed. O V λ1371.0 is absent in the spectra of HD 96715 and HD 168076, thus their temperature must be below 40,000 K. The lower limit to the temperature of these stars is established with P V $\lambda\lambda$1118.0,1128.0 and secondarily C IV $\lambda\lambda$1548.2,1550.8.

P V $\lambda\lambda$1118.0,1128.0 displays a wind profile (discrepant with the observed photospheric profile) in the models with $T_{\rm eff}\leq$37,000 K. In the 38,000 K to 42,000 K range all our models have an excess emission of C IV $\lambda\lambda$1548.2,1550.8 (with respect to the observations) but successfully fit the observed absorptions; however, at $T_{\rm eff}\leq$37,000 K the profile of the absorption changes (for any mass-loss rate) and does not fit the spectrum.

The $T_{\rm eff}$ of each object is determined from the best fit to the C IV λ1169+C III λ1176 and P V $\lambda\lambda$1118.0,1128.0 lines. We find $T_{\rm eff}$=41,000 K for HD 64568, $T_{\rm eff}$=40,000 K for HD 93250, HD 93205 and HDE 303308 and $T_{\rm eff}$=39,000 K for HD 96715 and HD 168076. The error bars given in Table 3 ($\pm$ 2,000 K) are larger than the range of acceptable temperatures of each object indicated by the spectra, because they also account for systematic errors, such as the uncertainty introduced by the flux normalization and the possible contribution by companions ($<$ 15%, see later) in some cases.

Once we delimit the effective temperature, we proceed to derive $\dot{M}$. Most of the lines useful for this purpose in the analysis of mid-O type stars (P V $\lambda\lambda$1118.0,1128.0, C IV λ1169+C III λ1176, N V $\lambda\lambda$1238.8,1242.8 and C IV $\lambda\lambda$1548.2,1550.8) are insensitive to the variation of $\dot{M}$ at the high temperatures of the early-O stars. The mass loss rate is then determined with the aid of the less prominent O V λ1371.0, N IV $\lambda\lambda$1718.0,1718.5, and Si IV $\lambda\lambda$1393.8,1402.8 (increasing with higher $\dot{M}$), and secondarily with O VI $\lambda\lambda$1031.9,1037.6 (decreasing with higher $\dot{M}$). For each object, the lower/upper limits to mass-loss rate are set to the values that produce O V λ1371.0 and N IV $\lambda\lambda$1718.0,1718.5 in defect/excess.

The most sensitive lines to $L_{\rm x}/L_{\rm bol}$ are O VI $\lambda\lambda$1031.9,1037.6 and N V $\lambda\lambda$1238.8,1242.8, as already noted in paper I. S VI $\lambda\lambda$933.4,944.52 is also sensitive, but it is given little weight in the fitting process as this region is heavily affected by the interstellar hydrogen absorption. N V $\lambda\lambda$1238.8,1242.8 presents a problem related to its unsaturated absorption (which we discuss in detail below) and cannot be used to constrain the shocks. $L_{\rm x}/L_{\rm bol}$ is then derived from the model that provides the best fit to O VI $\lambda\lambda$1031.9,1037.6, which increases with increasing shocks. In the range of temperatures and mass-loss rates we found for the dwarf stars, $L_{\rm x}/L_{\rm bol}$ must be comprised between -7.5 (minimum to reproduce the observed O VI profile) and -6.5 (when this line is in excess in the models, independently of the other stellar parameters), but can be further constrained for each object once $T_{\rm eff}$ and $\dot{M}$ are known (as reflected in Table 3).

We then calculated models with different radii (in the range 6-12 $R_{\odot}$) for log g =4.0. We find that if we increase the radius (i.e. we increase mass and luminosity), O VI $\lambda\lambda$1031.9,1037.6 increases while P V $\lambda\lambda$1118.0,1128.0, C III λ1176 and N IV $\lambda\lambda$1718.0,1718.5 decrease. At R_{*}=6$R_{\odot}$, the models do not reproduce the P Cygni profile of O VI. A model with a radius of R_{*}=12$R_{\odot}$ provides an overall worse fit to the spectra of HD 96715, HD 168076,

HDE 303308 and HD 93205 than R_*=9$R_\odot$. For these stars we adopt a radius of R_*=9$R_\odot$ $\pm$ 3 $R_\odot$ (HD 64568 and HD 93250 are discussed in Sections 5.1.2 and 5.1.3).

There is a limited number of photospheric lines sensitive to gravity in the FUSE and IUE ranges and, by consequence, the derived value of log g is less well constrained than the other stellar parameters. P V $\lambda\lambda$1118.0,1128.0 and N IV $\lambda\lambda$1718.0,1718.5 increase with decreasing gravity, and C III λ1176 has the opposite behavior. However, the strength of these lines depends on log g more weakly than on $T_{\rm eff}$ and $\dot{M}$. We find that models with log g =3.8 or 4.2 give poorer fits than log g =4.0 and we adopt these values as the error margin. Our findings agree with the results from works based on analyses of optical spectra that derive log g for HD 93205 and HDE 303308 between 3.9 and 4.1 (see Table 4) and with the calibration of log g with spectral type of Markova et al. (2004) and Vacca et al. (1996) that assign log g $\simeq$3.9 to O3 V and O4 V stars. For HD 168076, Morrison (1975) derived log g =4.3 from photometric data.

The best fit models are shown in Figures 5 and 6. The synthetic spectra reproduce with great accuracy most of the UV and Far-UV lines. Yet, they fail to reproduce the N V $\lambda\lambda$1238.8,1242.8 unsaturated profile in the *IUE* spectra of all stars. The *IUE* data may suffer from inaccurate background subtraction in this wavelength range due to the echelle order overlap (Bianchi & Bohlin 1984), so we searched for other UV spectra in the MAST archive. In Figures 2 and 6 we have included data in the N V $\lambda\lambda$1238.8,1242.8 region from *ORFEUS-TUES* for HD 96715 and from *HST-STIS* for HDE 303308 and HD 93205. The *ORFEUS-TUES* spectrum of HD 96715 displays a saturated N V $\lambda\lambda$1238.8,1242.8 P Cygni profile that the *WM-basic* model fits well, therefore at least in this case the mismatch is indeed likely to originate from the IUE data reduction. However, N V $\lambda\lambda$1238.8,1242.8 is unsaturated in the *STIS* spectra of both HDE 303308 and HD 93205. While the latter is a binary, thus the residual flux may originate from the cooler companion, the profile is hard to explain in HDE 303308. This prompted us to explore the grid of *WM-basic* models, to check if the combination of parameters that produces unsaturated N V $\lambda\lambda$1238.8,1242.8 overlaps with the range of parameters we found adequate for early type dwarf stars.

The behaviour of the N V $\lambda\lambda$1238.8,1242.8 doublet in models with log g = 4 and R_* = 9$R_\odot$ can be summarized as follows. It becomes stronger with increasing temperature up to $\sim$ 44,000 K (the exact value depends on $\dot{M}$ and $L_{\rm x}/L_{\rm bol}$) and then it decreases for $T_{\rm eff}\gtrsim$ 44,000 K. The doublet grows with increasing shocks up to log$L_{\rm x}/L_{\rm bol}$ $\leq$-6.75, then it decreases for log$L_{\rm x}/L_{\rm bol}$ $\geq$-6.75. In the range of temperatures we have determined for O3-4 V stars (38,000-42,000 K), higher $\dot{M}$ produces a stronger N V $\lambda\lambda$1238.8,1242.8 profile.

If we decrease $T_{\rm eff}$ so that the models produce unsaturated N V $\lambda\lambda$1238.8,1242.8, we canot reproduce the observed O VI $\lambda\lambda$1031.9,1037.6. If instead we increase $T_{\rm eff}$, we

achieve unsaturated C IV $\lambda\lambda$1548.2,1550.8 at lower $T_{\rm eff}$ (by 2,000 K) than needed to produce unsaturated N V $\lambda\lambda$1238.8,1242.8 (unsaturated C IV $\lambda\lambda$1548.2,1550.8 is in disagreement with the observed spectra of all dwarf stars except for HD 93250 and HD 64568). Reduced shocks underestimate O VI $\lambda\lambda$1031.9,1037.6. Model spectra calculated with lower mass-loss rate do not have N IV $\lambda\lambda$1718.0,1718.5. We can fit N V $\lambda\lambda$1238.8,1242.8 in the spectra of HD 93205 and HDE 303308 (but not HD 93250) with a nitrogen abundance of $\epsilon_N = 0.1\ \epsilon_{N,\odot}$ but the models lack N IV $\lambda\lambda$1718.0,1718.5 (see Figure 6). Note that none of the stars analysed in this work is in the OBC/OBN compilation of Walborn (1976), nor we found any publication that measured non-solar compositions for them.

In conclusion, we cannot compute a *WM-basic* model that displays unsaturated N V $\lambda\lambda$1238.8,1242.8 and is in agreement with the rest of the observed spectrum. We suspect that a shock (and X-ray ionization) treatment different from what used by WM-basic may reproduce the N V $\lambda\lambda$1238.8,1242.8 P Cygni profile. We will investigate this possibility by comparing models computed with WM-basic and CMFGEN (Bianchi, Garcia, & Herald (2003), Bianchi, Garcia, & Herald, in preparation).

5.1.1. HD 93205 and HD 168076

There is an additional source of uncertainty in the analysis of HD 93205 and HD 168076. Both of them are binaries whose secondary component is most likely included in the FUSE and IUE apertures, its contribution to the observed total flux being however hard to quantify.

The secondary component of HD 93205 is an O8 V star. From our grid of synthetic spectra we know that the O8 V continuum flux ($T_{\rm eff}$=30,000 K, from Figure 8) can be up to 50% the flux of an O3.5 V ($T_{\rm eff}$=40,000 K, this work) in the 900-1800Å range if the stars had the same radius. Yet, we can narrow down this upper limit. N V $\lambda\lambda$1238.8,1242.8 is almost absent in the UV spectrum of O8 V stars (Walborn, Nichols-Bohlin, & Panek 1985). If we assume that this line is saturated in O3.5 V stars (see, for example, the *ORFEUS* spectrum of HD 96715 in Figure 2) the residual flux at its core in the IUE spectrum, of $\sim$ 15%, may originate from the secondary and/or inaccurate background subtraction, as explained previously. As for other lines, the spectrum of an O8 V star displays photospheric profiles of Si IV $\lambda\lambda$1393.8,1402.8 and N IV $\lambda\lambda$1718.0,1718.5, and unsaturated C IV $\lambda\lambda$1548.2,1550.8 (Walborn, Nichols-Bohlin, & Panek 1985). This could explain the subtle mismatch of the best fit model to the observed emission of C IV $\lambda\lambda$1548.2,1550.8 and the absorptions of Si IV $\lambda\lambda$1393.8,1402.8 and N IV $\lambda\lambda$1718.0,1718.5.

The HD 168076 system is much less known. Since we do not know the spectral type of

the secondary component, we cannot speculate the contamination to the O4 V((f)) star UV and Far-UV spectra. These, however, are very similar to the spectra of the other dwarves in the sample, therefore the contribution from the secondary cannot be conspicuous. A possible effect from the secondary is that the N V $\lambda\lambda$1238.8,1242.8 and C IV $\lambda\lambda$1548.2,1550.8 features are not saturated. Again, if we suppose that these lines are saturated in the spectrum of the main component, we can estimate the contribution of the secondary to be $\lesssim 10\%$ to the total flux in the *IUE* range.

5.1.2. HD 93250

The *IUE* spectrum of HD 93250 displays an unsaturated C IV $\lambda\lambda$1548.2,1550.8 P Cygni profile. This feature was noted by Walborn, Nichols-Bohlin, & Panek (1985) who suggested that it may indicate a hidden companion. Yet, the star has not been found to be binary (see Section 3). A poor background subtraction in the IUE spectrum may make N V $\lambda\lambda$1238.8,1242.8 appear unsaturated, but not C IV $\lambda\lambda$1548.2,1550.8 (Bianchi & Bohlin 1984). Our grid of models shows C IV $\lambda\lambda$1548.2,1550.8 not saturated when $R_*\geq 12R_\odot$ and $T_{\rm eff}\gtrsim$42,000 K (the actual temperature depends on R_* and $\dot{M}$). Note that a large radius would be consistent with the high luminosity of this object.

We studied the behaviour of the main lines (C III, C IV, N IV, N V, O V, O VI and P V) in a wide range of temperatures, mass-loss rates and $L_{\rm x}/L_{\rm bol}$ values, ([37,000, 50,000] K, [$2{\cdot}10^{-7}$,$1{\cdot}10^{-6}$]$M_\odot$ yr^{-1}, [-6.75,-8.0]) in search of intervals where we can reproduce simultaneously all the strongest features of the spectrum of HD 93250 and the unsaturated profile of C IV $\lambda\lambda$1548.2,1550.8.

We find that the lower the mass-loss rate, the lower is the temperature where models display unsaturated C IV $\lambda\lambda$1548.2,1550.8. In models with R_*=12$R_\odot$, independently of the value of shocks, C IV $\lambda\lambda$1548.2,1550.8 becomes unsaturated at $T_{\rm eff}$=42,000/45,000/49,000 K for $\dot{M}$=$2{\cdot}10^{-7}$/$5{\cdot}10^{-7}$/$1{\cdot}10^{-6}$$M_\odot$ yr^{-1}. However, the upper limit to $T_{\rm eff}$ set by N IV $\lambda\lambda$1718.0,1718.5 and O VI $\lambda\lambda$1031.9,1037.6 is lower (by $\sim$2,000/4,000/6,000 K and 4,000/7,000/9,000 K respectively, for $L_{\rm x}/L_{\rm bol}$ =-6.75) than required for the unsaturated C IV $\lambda\lambda$1548.2,1550.8. If instead we decrease shocks for an intermediate mass-loss rate of $\dot{M}$=$5{\cdot}10^{-7}$$M_\odot$ yr^{-1}, the temperature required to fit O VI $\lambda\lambda$1031.9,1037.6 and N IV $\lambda\lambda$1718.0,1718.5 increases by 1,000 K for every drop of $\Delta \log L_{\rm x}/L_{\rm bol}$ =-0.5 while it remains constant for C IV $\lambda\lambda$1548.2,1550.8. Therefore in models with $T_{\rm eff}\sim$42,000 K and low $\dot{M}$ and $L_{\rm x}/L_{\rm bol}$ this gap would be reconciled. However, other prominent lines (O V λ1371.0, P V $\lambda\lambda$1118.0,1128.0 and C III λ1176) are not reproduced. We conclude that we cannot fit the observed C IV $\lambda\lambda$1548.2,1550.8 consistently with the rest of the spectral lines.

We find the best solution to be $\log L_{\rm x}/L_{\rm bol}$ =-7.25, $\dot{M}$=5.5·10^{-7}M$_\odot$ yr^{-1}, $T_{\rm eff}$=40,000 K, R_*= 12$R_\odot$ and log g =4. With these parameters the model reproduces O VI $\lambda\lambda$1031.9,1037.6, P V $\lambda\lambda$1118.0,1128.0, C III λ1176, O V λ1371.0 and N IV $\lambda\lambda$1718.0,1718.5 (see Figures 5 and 6). This model however, has saturated profiles of N V $\lambda\lambda$1238.8,1242.8 and C IV $\lambda\lambda$1548.2,1550.8, in disagreement with the observed spectrum. Because C III λ1176 is well fit, a different carbon abundance would not improve the solution. As seen in Section 5.1, N V $\lambda\lambda$1238.8,1242.8 is always saturated in the range of parameters considered for solar abundances, and models underabundant in nitrogen are incompatible with N IV $\lambda\lambda$1718.0,1718.5. The non-saturated absorptions of C IV $\lambda\lambda$1548.2,1550.8 and N V $\lambda\lambda$1238.8,1242.8 may be due to an unresolved cooler companion.

5.1.3. HD 64568

The only IUE spectrum of HD 64568 has low dispersion. The stellar parameters are therefore constrained primarily with lines in the FUSE range. By consequence, the uncertainty of the derived $\dot{M}$ and $L_{\rm x}/L_{\rm bol}$ is higher than for the other objects of the sample, as we explain below. This is not the case for v_∞ (derived from O VI $\lambda\lambda$1031.9,1037.6) or log g (determined with C III λ1176 and P V $\lambda\lambda$1118.0,1128.0, but highly uncertain among the sample dwarf stars), which are entirely determined from the high resolution *FUSE* spectrum. The effective temperature is well constrained with C III λ1176 and P V $\lambda\lambda$1118.0,1128.0. These lines in HD 64568 are the weakest in our sample indicating higher $T_{\rm eff}$ (41,000 K), in accordance with its earliest spectral type.

C IV $\lambda\lambda$1548.2,1550.8 is unsaturated. At the star's effective temperature, the models (degraded to the [low] resolution of the observed spectrum) only display unsaturated C IV $\lambda\lambda$1548.2,1550.8 if $\dot{M}\leq$ 2·10^{-7}M$_\odot$ yr^{-1}, R_*>12$R_\odot$ and $\log L_{\rm x}/L_{\rm bol} > -7.0$. C IV $\lambda\lambda$1548.2,1550.8 decreases with larger radii and, together with O VI $\lambda\lambda$1031.9,1037.6, helps us constrain this parameter. We set the upper limit for the radius to 16$R_\odot$, when the models display O VI $\lambda\lambda$1031.9,1037.6 in excess regardless of the other stellar parameters, and the lower limit to 12$R_\odot$, when they cannot produce unsaturated C IV $\lambda\lambda$1548.2,1550.8.

The mass-loss rate and shocks were determined as explained in Section 5.1. Since most of the $\dot{M}$ indicators (O V λ1371.0, Si IV $\lambda\lambda$1393.8,1402.8 and N IV $\lambda\lambda$1718.0,1718) are in the *IUE* range, the derived mass-loss rate of HD 64568 is highly uncertain. The derived $L_{\rm x}/L_{\rm bol}$, though determined from O VI $\lambda\lambda$1031.9,1037.6 in the *FUSE* range, is affected by the uncertainty in $\dot{M}$, since the strength of the doublet also depends on mass-loss rate.

5.2. *The Supergiant Star, HD 190429A*

The spectrum of the O4 supergiant displays very strong lines which, in comparison to the spectra of the mid-O supergiant stars analysed in paper I (see Section 4.2), denote higher temperature and mass-loss rate. In particular, the prominent He II λ1640.0 emission line indicates, according to our grid of models, that the mass-loss rate is higher than $7 \cdot 10^{-6} M_\odot$ yr^{-1} .

In the range of temperatures and mass-loss rates we considered for HD 190429A (35,000-40,000 K and $3.\cdot 10^{-6}$ -$1.5\cdot 10^{-5} M_\odot$ yr^{-1}, as suggested by the star's spectral morphology), C III λ1176, P V $\lambda\lambda$1118.0,1128.0 and Si IV $\lambda\lambda$1393.8,1402.8 increase with increasing $\dot{M}$ and with decreasing $T_{\rm eff}$ and $L_{\rm x}/L_{\rm bol}$ (similarly to what we found in paper I). He II λ1640 has the same dependence on $\dot{M}$ and $T_{\rm eff}$ but does not vary appreciably with $L_{\rm x}/L_{\rm bol}$. The effective temperature is constrained from C III λ1176 and Si IV $\lambda\lambda$1393.8,1402.8. For $T_{\rm eff} \leq$ 36,000 K the models with $\dot{M} > 7 \cdot 10^{-6} M_\odot$ yr^{-1} display a P Cygni profile of C III λ1176, not seen in the observed spectrum. For $T_{\rm eff} \geq$ 39,000 K, C III λ1176 and Si IV $\lambda\lambda$1393.8,1402.8 are absent even in models with mass-loss rate as high as $\dot{M} \sim 1.4 \cdot 10^{-5}$ $M_\odot$ yr^{-1}, thus providing an upper limit to $T_{\rm eff}$. In this range of temperatures, the models reproduce He II λ1640.0 for $\dot{M} \geq 1.0 \cdot 10^{-5}$ $M_\odot$ yr^{-1} (lower limit of mass-loss rate). Models with $\dot{M} \geq 1.4 \cdot 10^{-5}$ $M_\odot$ yr^{-1} (upper limit) display excessive P V $\lambda\lambda$1118.0,1128.0 profiles. The shocks in the wind were determined by fitting O VI $\lambda\lambda$1031.9,1037.6 and O V λ1371.0 (both oxygen lines increase with increasing shocks) and Si IV $\lambda\lambda$1393.8,1402.8. In addition, different values of $L_{\rm x}/L_{\rm bol}$ change the shape of the P V $\lambda\lambda$1118.0,1128.0 absorptions.

In this regime of $T_{\rm eff}$ and $\dot{M}$, the models with $R_* \geq 23$ $R_\odot$ produce unsaturated C III λ1176 thus setting the lower limit of R_*. The upper limit is $27 R_\odot$ because models with larger radius produce O VI $\lambda\lambda$1031.9,1037.6 stronger than observed regardless of the other stellar parmeters. Other lines sensitive to the radius, which helped us to further contrain its value, are He II λ1640.0 and Si IV $\lambda\lambda$1393.8,1402.8 (which decrease with increasing radius) and O V λ1371.0 (favoured by larger radii); the profile of P V $\lambda\lambda$1118.0,1128.0 +Si IV $\lambda\lambda$1122.5,1128.3,1128.4 also changes with radius.

Contrary to what we find for the dwarf stars, almost all the spectral lines are sensitive to gravity, and we can use them to derive $\log g$. Higher $\log g$ corresponds to weaker O VI $\lambda\lambda$1031.9,1037.6, O V λ1371.0 and He II λ1640.0, while Si IV $\lambda\lambda$1393.8,1402.8 increases and the aborption of P V $\lambda\lambda$1118.0,1128.0 grows deeper. The carbon lines are also affected by an increase of $\log g$: C IV $\lambda\lambda$1548.2,1550.8 decreases and the absorption of C IV λ1169+C III λ1176 increases whereas its emission diminishes.

We find the best fit at $T_{\rm eff}$=37,500 K, $\log g = 3.4$, $R_* = 25 R_\odot$, $\dot{M} = 1.2 \cdot 10^{-5}$ $M_\odot$ yr^{-1},

$\log L_{\rm x}/L_{\rm bol}$ = -6.5 , $L_{\rm bol}$=6.05 and v_∞= 2100 km s^{-1}. This model reproduces most of the wind features (see Figure 7) including the lines of O IV, O VI, P V+Si IV, C IV, Si IV, He II and N IV. Minor discrepancies remain in the fit to some of these lines, which can be attributed to the contribution of the secondary to the flux of the system. Even though the lines used for the analysis come primarily from the O4 star, they may have a residual flux in the absorption trough from the O9.5 II companion. The comparison of spectra from the IUE atlas of stars (Walborn, Nichols-Bohlin, & Panek 1985) of O4 I stars (main component) and O9.5 II stars (companion) provides an upper limit for the contribution of the secondary. An O9.5 bright giant displays weak N V $\lambda\lambda$1238.8,1242.8 while the doublet has typically a saturated absorption in an O4 I star. From the depth of N V $\lambda\lambda$1238.8,1242.8 in the IUE spectrum of the system we estimated that the companion may amount to $\lesssim$ 15% of the total. The O9.5 II star has strong Si IV $\lambda\lambda$1393.8,1402.8; this would explain why Si IV $\lambda\lambda$1393.8,1402.8 is weaker in our models than observed. C IV $\lambda\lambda$1548.2,1550.8 is fully developed but not saturated in the O9.5 II star, which would explain the excess emission and absorption of the model. The spectrum of an O9.5 II has weak photospheric N IV $\lambda\lambda$1718.0,1718.5, and this makes the P Cygni profile from the O4 If$^+$ star look less developed (relative to the total continuum), thus this line appears slightly in excess in the model.

In the FUSE range, according to the Copernicus atlas of OB stars of Walborn & Bohlin (1996), an O9.5 II star has photospheric S IV $\lambda\lambda$1062.7,1073.0,1073.5, and P V $\lambda\lambda$1118.0,1128.0 +Si IV $\lambda\lambda$1122.5,1128.3,1128.4 lines, which will increase the depth of the O4 If$^+$ wind lines. O VI $\lambda\lambda$1031.9,1037.6 and C IV λ1169+C III λ1176 have unsaturated P Cygni profiles in O9.5 II stars, possibly causing the mismatch of the best fit model to these lines.

However, there is another explanation for the discrepancies. It is possible that HD 190429A has non solar surface abundances. In Figure 7 we present a model with modified CNO abundances ($\epsilon_{He} = 5\ \epsilon_{He,\odot}$, $\epsilon_C = 0.5\ \epsilon_{C,\odot}$, $\epsilon_N = 2.0\ \epsilon_{N,\odot}$, $\epsilon_O = 0.1\ \epsilon_{O,\odot}$), which would be compatible with a scenario where HD 190429A is evolving towards the Wolf-Rayet phase, as suggested by previous authors (see Section 3). The modified CNO abundances improve the fit to C IV λ1169+C III λ1176 and the oxygen lines (O VI $\lambda\lambda$1031.9,1037.6, O IV $\lambda\lambda$1339.0,1343.0 and O V λ1371.0) but degrades the fit to P V $\lambda\lambda$1118.0,1128.0 and Si IV $\lambda\lambda$1393.8,1402.8.

There is one feature, S IV $\lambda\lambda$1062.7,1073.0,1073.5, definitely produced in the primary star spectrum, that the *WM-basic* models do not reproduce. We encountered the same problem when we modeled the spectra of the mid-O type supergiant stars in paper I. The S IV $\lambda\lambda$1062.7,1073.0,1073.5 problem is probably due to the atomic data used in *WM-basic* and prompted a comparison with models computed with the Hillier & Miller (1998) *CMFGEN* code. The synthetic spectra generated with both codes for an equivalent set of stellar parameters display very similar photospheric and wind features with the exception of

S IV $\lambda\lambda$1062.7,1073.0,1073.5 (Bianchi, Garcia, & Herald (2003); Bianchi, Garcia, & Herald, in preparation). *WM-basic* and *CMFGEN* predict very different ionization fractions for sulphur.

6. SUMMARY AND DISCUSSION

We have performed a detailed spectroscopic analysis of seven Galactic early-O type stars and derived their stellar parameters. We found effective temperatures ranging from 41,000 K to 39,000 K for the O3-4 dwarf stars and 37,500 K for the O4 supergiant. The X-ray ionization due to shocks in the wind has been constrained by our modeling, primarily from the O VI $\lambda\lambda$1031.9,1037.6 resonance doublet, accessible with the *FUSE* telescope. In the range of $T_{\rm eff}$, $\dot{M}$ and R_* that we derived for the dwarf stars, the spectral morphology hardly changes with gravity and the derived value of log g is less well constrained than other parameters, but consistent with previous estimates.

All the sample stars display unsaturated N V $\lambda\lambda$1238.8,1242.8 profiles that we cannot fit consistently with the rest of the spectrum. In one case at least (HD 96715), the unsaturated profile is due to poor background subtraction in the IUE data (as shown by an *ORFEUS* spectrum), and this may apply to the other stars as well. In the case of HD 190429A, HD 93205 and HD 168076, the unsaturated profile may also be due to flux from the cooler companion star, whose contribution we estimate to be $\leq$ 15% of the observed flux. A comparison of *WM-basic* and *CMFGEN* models calculated with parameters suitable for the early-O type stars is under way (Bianchi, Garcia, & Herald (2003); Bianchi, Garcia, & Herald, in preparation), to investigate the effect of a different treatement of the shocks on the N V $\lambda\lambda$1238.8,1242.8 doublet.

We compile previous determinations of the stellar parameters for our program stars from the literature in Table 4. Our effective temperatures are consistently lower than those derived in other works, with the only exception of the Strömgren and Hβ photometric studies by Kaltcheva & Georgiev (1993) and Salukvadze & Javakhishvili (1995). Kaltcheva & Georgiev (1993) derived temperatures for the Carina stars of our sample lower than ours by $\sim$4,000 K on average. Salukvadze & Javakhishvili (1995) assigned a temperature of 28,200 K to HD 190429 (without resolving the system), closer to what we would expect for the secondary than to what we found for HD 190429A (37,500 K). Morrison (1975) performed Strömgren and Hβ photometry of HD 168076 and derived a temperature higher than ours by 16,000 K. The calibration of Conti (1975), based on the comparison of the equivalent widths of hydrogen and helium lines with plane-parallel hydrostatic non-LTE model predictions, was used by Conti & Walborn (1976) and Conti & Frost (1977) for several objects

of our sample, yielding temperatures higher than our results by > 10,000 K. Temperatures obtained from fitting Balmer lines and optical He I and He II lines with plane-parallel non-LTE hydrostatic models are ∼ 10% (Simon et al. 1983) to ∼20% (Kudritzki et al. 1992; Puls et al. 1996) higher than ours. Pauldrach, Hoffmann, & Lennon (2001) compared the *IUE* spectrum of HD 93250 to *WM-basic* models of $T_{\rm eff}$=50,000 K (approximately the same as derived by Puls et al. (1996)), log g =4.0 and R_*=12$R_\odot$, with different mass-loss rates around $\dot{M}$=5.6·10^{-6}M$_\odot$ yr^{-1}. Their synthetic spectra did not include shocks effects and either produce O V λ1371.0 in excess or cannot reproduce the N IV $\lambda\lambda$1718.0,1718.5 line. In our work we used those lines, together with C IV λ1169+C III λ1176 and P V $\lambda\lambda$1118.0,1128.0, to set the upper limit of the effective temperature of the dwarf stars to ∼42,000 K (see Section 5) and we obtained a consistent fit of all spectral features by including the effects of shocks in the calculations.

In Figure 8 we compare the effective temperatures and luminosities obtained for the total sample of O3-O7 type stars analysed in this work and in paper I with previous empirical calibrations (Vacca et al. (1996), de Jager & Nieuwenhuijzen (1987) and Markova et al. (2004)). Our $T_{\rm eff}$ values for O3-O6 dwarf stars are lower than these calibrations, the differences ranging between 9,000-10,000 K, 6,000-9,000 K and 4,000-7,000 K respectively. The discrepancy is smaller for the O4-O7 supergiants (6,000-10,000 K, 4,000-6,000 K and 2,000-3,500 K, respectively). The derived luminosities for both dwarf stars and supergiants are also lower, by an average of 7% and 10% respectively, than both the calibrations of de Jager & Nieuwenhuijzen (1987) and Vacca et al. (1996). For the O4 If$^+$ supergiant the luminosity is also lower, but the discrepancy is within the error bars.

The lower temperatures from our analysis are due to two main improvements. On the one hand, the use of *FUSE* data enables the assessment of X-rays from shocks and thus a correct (consistent) derivation of the wind ionization. On the other hand, the inclusion of line-blanketing effects in the analysis yields lower effective temperatures than pure hydrogen and helium model analyses. Optical spectra analyses of massive stars with spherical, hydrodynamic, wind-blanketed, non-LTE synthetic spectra also revised the temperature scale downwards (Martins, Schaerer, & Hillier 2002; Herrero, Puls, & Najarro 2002; Repolust et al. 2003). Our derived $T_{\rm eff}$ values are still lower. Temperatures of O3 V and O4 V stars, according to the scale of Martins, Schaerer, & Hillier (2002) (based on calculations with the CMFGEN code) are ≃47,500 K and ≃44,500 K, whereas we have obtained 41,000 K and 40,000-39,000 K. From the work of Herrero, Puls, & Najarro (2002), who fit Balmer, He I and He II optical lines with FASTWIND (Santolaya-Rey, Puls, & Herrero 1997), we can interpolate a temperature of 41,250 K for an O4 If$^+$, i.e. ∼4,000 K higher than we derived for HD 190429A. Repolust et al. (2003), proceeding similarly, obtained 46,000 K for HD 93250 (in contrast with our result, 40,000 K) and 41,000 K for HDE 303308 (in agreement within

the error bars with our value, 40,000 K). The remaining disagreement between these results and ours may originate in the fact that the analyses are based on optical and UV data respectively. We are planning to analyse optical spectra of the sample stars to check the consistency of our results from the UV and Far-UV.

The spectral lines in the FUSE and IUE ranges constrain $\dot{M}$ as well. The mass-loss rate we derived for HD 190429A ($1.2{\cdot}10^{-5}$M$_\odot$ yr^{-1}) agrees with the values derived from Hα by Conti & Frost (1977) ($1.1 \cdot 10^{-5}$M$_\odot$ yr^{-1}), Leitherer (1988) ($1.26{\cdot}10^{-5}$M$_\odot$ yr^{-1}), Scuderi et al. (1992) ($8.6{\cdot}10^{-6}$M$_\odot$ yr^{-1}) and Markova et al. (2004) ($1.42 \cdot 10^{-5}$M$_\odot$ yr^{-1}). Studies of IR and radio spectra yield lower $\dot{M}$: $4.6 \cdot 10^{-6}$M$_\odot$ yr^{-1} (Scuderi et al. 1998, radio), $<0.35{\cdot}10^{-6}$M$_\odot$ yr^{-1}(Persi, Ferrari-Toniolo, & Grasdalen 1983, IR). For the dwarf stars the mass-loss rates derived in the literature are at least one order of magnitude higher than ours. For HD 93250, the exceptionally high value of $\dot{M}$=$4.1 \cdot 10^{-5}$ (Leitherer, Chapman, & Koribalski 1995) was determined from radio fluxes at 8.54 GHz, but the data may be contaminated by non-thermal emission; for this object, there is also one measurement lower than ours by one order of magnitude. In view of the systematic differences for dwarf stars, we used the "recipe" of Vink, de Koter, & Lamers (2000), based on the radiation pressure driven wind theory, to predict the mass-loss rates of the sample stars from their derived photospheric parameters. The predictions are presented in Table 3. The mass-loss rate derived for HD 190429A agrees with the prediction. For dwarf stars our values are lower than predicted by a factor of $\sim$2 ($\sim$4 for HD 64568).

In general, the stellar masses we have obtained are lower than values determined in previous works, as shown in Table 4. In the case of HD 93205, the mass had been derived from the orbital parameters of the binary system: $M_*\geq$ 31.5 (Morrell et al. 2001), $M_*\geq$ 32.6 (Stickland & Lloyd 1993), $M_*\geq$ 37 (Corti, Albacete, Morrell, & Niemela 1999). For this star we derive $30{\pm}10M_\odot$, lower than previous determinations but compatible within the errors. The primary mass yields a mass of the secondary of $13{\pm}5M_\odot$ for a mass ratio of q=0.423 (Morrell et al. 2001), a mass significantly lower than derived for other O8 V stars in eclipsing systems like, for example, DN Cas, for which Brancewicz & Dworak (1980) give $24M_\odot$. However, it must be emphasized here that the uncertainty in log g and R_* (see Section 5.1) makes the derived value of the stellar masses much more uncertain than other parameters (like $T_{\rm eff}$ and $\dot{M}$). Hopefully the mass determination will be refined with a consistent analysis of optical spectra, planned as a future work.

Our results improve the empirical calibration of the Wind momentum-Luminosity Relation (WLR). The WLR relates the so-called modified wind momentum $D_{mom} = \dot{M}v_\infty(R_*/R_\odot)^{0.5}$ to the luminosity of the star as $D_{mom} \propto L^x$ (Kudritzki, Lennon, & Puls 1995). In the past few years a big effort has been made to calibrate the WLR (Puls et al. 1996; Kudritzki &

Puls 2000; Herrero, Puls, & Najarro 2002; Repolust et al. 2003; Markova et al. 2004) for its promising application to distance determinations. In Figure 9 we plot the WLR for the total sample of stars studied in this paper and in paper I. Our points are mostly consistent with the theoretical relation of Vink, de Koter, & Lamers (2000) within the error bars.

We are planning to extend our modeling of Far-UV and UV spectra to a larger sample of O type stars and to the optical range. The lower $T_{\rm eff}$ values (compared with previous results/calibrations) have great implications for understanding the ionisation of HII regions, since cooler stars would produce less photons energetic enough to ionize hydrogen ($\lambda <$ 912Å). For instance, the ionizing flux from a star of $T_{\rm eff}$=40,000 K amounts to only 30% of the flux from a $T_{\rm eff}$=50,000 K star with the same radius.

We are indebted to Adi Pauldrach for assisting us with the use of the *WM-basic* code. This work is based on data obtained by the NASA-CNES-CSA *FUSE* mission operated by the Johns Hopkins University. The data from the *IUE* satellite presented in this paper were obtained from both the INES archive and the Multimission Archive at the Space Telescope Science Institute (MAST). Financial support has been provided in part by NASA grants NAS5-32985 and NRA-99-01-LTSA-029.

REFERENCES

Abbott, D. C., Bieging, J. H., Churchwell, E., & Cassinelli, J. P. 1980, ApJ, 238, 196

Abt, H. A. 1986, ApJ, 304, 688

Antokhina, E. A., Moffat, A. F. J., Antokhin, I. I., Bertrand, J., & Lamontagne, R. 2000, ApJ, 529, 463

Benvenuto, O. G., Serenelli, A. M., Althaus, L. G., Barbá, R. H., & Morrell, N. I. 2002, MNRAS, 330, 435

Bianchi, L. et al. 2000, ApJ, 538, L57

Bianchi, L., & Garcia, M. 2002, ApJ, 581, 610 (*paper I*)

Bianchi, L., Garcia, M., & Herald, J. 2003, Revista Mexicana de Astronomia y Astrofisica Conference Series, 15, 226

Bianchi, L., Garcia, M., & Herald, J. 2004, in preparation

Bianchi, L. & Bohlin, R.C. 1984, A&A, 134, 31

Bohlin, R. C., Savage, B. D., & Drake, J. F. 1978, ApJ, 224, 132

Bosch, G. L., Morrell, N. I., & Niemelä, V. S. 1999, RMxAA, 35, 85

Brancewicz, H. K. & Dworak, T. Z. 1980, Acta Astronomica, 30, 501

Chlebowski, T., Harnden, F. R. Jr, & Sciortino, S. 1989, ApJ, 341, 427

Chlebowski, T. & Garmany, C. D. 1991, ApJ, 368, 241

Conti, P. S. 1975, LNP Vol. 42: H II regions and related topics, 207

Conti, P. S., & Alschuler, W. R. 1971, ApJ, 170, 325

Conti, P. S., & Frost, S. A. 1977, ApJ, 212, 728

Conti, P. S., & Leep, E. M. 1974, ApJ, 193, 113

Conti, P. S. & Walborn, N. R. 1976, ApJ, 207, 502

Conti, P. S. & Garmany, C. D. 1980, ApJ, 238,190

Conti, P. S., Hanson, M. M., Morris, P. W. et al. 1995, ApJ, 445, L35

Corti, M., Albacete, F., Morrell, N. I., & Niemela, V. S. 1999, Revista Mexicana de Astronomia y Astrofisica Conference Series, 8, 137

Crampton, D. 1971, AJ, 76, 260

Crampton, D. 1972, MNRAS,158, 85

Cruz-Gonzalez, C., Recillas-Cruz, E., Costero. R., Peimbert, M., & Torres-Peimbert, S. 1974, RMxAA, 1, 211

Diplas, A. & Savage, B. D. 1994, ApJS, 93, 211

Dixon, V., Kruk, J. & Murphy, E. 2001: "The CalFUSE Pipeline Reference Guide", available only electronically at http://fuse.pha.jhu.edu/analysis/pipeline_reference.html

Doom, C. & de Loore, C. 1984, ApJ, 278, 695

Duchêne, G., Simon, T., Eislöffel, J., & Bouvier, J. 2001, A&A, 379, 147

Feinstein, A., Marraco, H. G., & Muzzio, J. C. 1973, A&AS, 12, 331

Feinstein, A. 1982, AJ, 87, 1012

Garmany, C. D., Olson, G. L., van Steenberg, M. E., & Conti, P. S. 1981, ApJ, 250, 660

Garrison, R. F., Hiltner, W. A., & Schild, R. E. 1977, ApJS, 35, 111

van Genderen, A. M. et al. 1989, A&AS, 79, 263

van Genderen, A. M. 2003, A&A, 397, 921

Guetter, H. H. 1968, PASP, 80, 197

Havlen, R. J. 1972, A&A, 17, 413

Herrero, A., Puls, J., & Najarro, F. 2002, A&A, 396, 949

Hillenbrand, L. A., Massey, P., Strom, S. E., & Merril, K. M. 1993, AJ, 106, 1906

Hillier, D. J. & Miller, D. L. 1998, ApJ, 496, 407

Houk, N. & Smith-Moore, M. 1988, Michigan Spectral Survey, Ann Arbor, Dept. of Astronomy, Univ. Michigan (Vol. 4) (1988) Available electronically at: http://cdsweb.u-strasbg.fr/cgi-bin/qcat?III/133

Howarth, I. D., Siebert, K. W., Hussain, G. A. J., & Prinja, R. K. 1997, MNRAS, 284, 265

de Jager, C., & Nieuwenhuijzen, H. 1987, A&A, 177, 217

Kaltcheva, N. T. & Georgiev, L. N. 1993, MNRAS, 261, 847

Kaltcheva, N. T. & Hilditch, R. W. 2000, MNRAS, 312, 753

Kudritzki, R.-P. 1980, A&A, 85, 174

Kudritzki, R.-P., Hummer, D. G., Pauldrach, A. W. A., Puls, J., Najarro, F., & Imhoff, J. 1992, A&A, 257, 655

Kudritzki, R.-P., Lennon, D. J., & Puls, J. 1995, In: Walsh J.R., Danziger, I.J. (eds.) Science with the VLT. Springer Verlag, p246

Kudritzki, R. & Puls, J. 2000, ARA&A, 38, 613

Lamers, H. J. G. L. M., Snow, T. P., & Lindholm, D. M. 1995, ApJ, 455, 269

Lee, D., Min, K., Dixon,W. V. D., Hurwitz, M., Ryu, K., Seon, K., & Edelstein, J. 2000, ApJ, 545, 885

Leitherer, C. 1988, ApJ, 326, 356

Leitherer, C., Chapman, J. M., & Koribalski, B. 1995, ApJ, 450, 289

Levato, H. & Malaroda, S. 1982, PASP, 94, 807

Levato, H., Malaroda, S., Morrell, N., Garcia, B., & Hernandez, C. 1991, ApJS, 75, 869

Lodén, L. O. 1965, ApJ, 141, 668

MacConnell, D. J., & Bidelman, W. P. 1976, AJ, 81, 225

Markova, N., Puls, J., Repolust, T., & Markov, H. 2004, A&A, 413, 693

Martins, F., Schaerer, D., & Hillier, D. J. 2002, A&A, 382, 999

Mason, B. D., Gies, D. R., Hartkopf, W. I., Bagnuolo, W. G. Jr et al. 1998, AJ, 115, 821

Massey, P. 1998, Stellar astrophysics for the local group: VIII Canary Islands Winter School of Astrophysics, 95

Mathys, G. 1988, A&AS, 76, 427

Moos, H. W., Cash, W. C., Cowie, L. L., Davidsen, A. F., et al. 2000, ApJ, 538, L1

Morgan, W. W., Whitford, A. E., & Code, A. D. 1953, ApJ, 118, 318

Morgan, W. W., Code A. D., & Whitford A. E. 1955, ApJS, 2, 41

Morrell, N. I. et al. 2001, MNRAS, 326, 85

Morris, P. W., Eenens, P. R. J., & Blum, R. D. et al. 1996, ApJ, 470, 597

Morrison, N. D. 1975, ApJ, 200, 113

Oke, J. B. 1954, ApJ, 120, 22

Pauldrach, A.W.A., Hoffmann, T. L. & Lennon, M. 2001, A&A, 375, 161

Pellerin, A., Fullerton, A.W., Robert, C., Howk, J.C., Hutchings, J.B., Walborn, N.R., Bianchi, L., Crowther, P.A., and Sonneborn, G. 2002, ApJS, 143, 159

Penny, L.R., Gies, D.R., and Bagnuolo, W.G.Jr 1996, ApJ, 460, 906

Persi, P., Ferrari-Toniolo, M., & Grasdalen, G. L. 1983, ApJ, 269, 625

Peton-Jonas, D. 1981, A&AS, 45, 193

Puls, J., Kudritzki, R. P., Herrero, A., Pauldrach, A. W. A., et al. 1996, A&A, 305, 171

Rachford, B. L. et al. 2002, ApJ, 577, 221

Repolust, T., Puls, J., & Herrero, A. 2003, A&A, accepted

Sahnow, D., Moos, H. W., Ake, T. B. et al. 2000, ApJ, 538, L7

Sahnow, D. 2002: "The FUSE Instrument and Data Handbook", available only electronically at http://fuse.pha.jhu.edu/analysis/IDH/IDH.html

Salukvadze, G. N. & Javakhishvili, G. S. 1995, Astronomische Nachrichten, 316, 275

Santolaya-Rey, A. E., Puls, J., & Herrero, A. 1997, A&A, 323, 488

Schaller, G., Schaerer, D., Meynet, G., & Maeder, A. 1992, A&AS, 96, 269

Schild, R. E., Garrison, R. F., & Hiltner, W. A. 1983, ApJS, 51, 321

Schild, H. & Berthet, S. 1986, A&A, 162, 369

Scuderi, S., Bonanno, G., di Benedetto, R., Spadaro, D., & Panagia, N. 1992, ApJ, 392, 201

Scuderi, S., Panagia, N., Stanghellini, C., Trigilio, C., & Umana, G. 1998, A&A, 332, 251

Seward, F. D. & Chlebowski, T. 1982, ApJ, 256, 530

Simon, K. P., Kudritzki, R. P., Jonas, G., & Rahe, J. 1983, A&A, 125, 34

Sharpless, S. 1959, ApJS, 4, 257

Solivella, G. R., & Niemela, V. S. 1986, RMxAA, 12, 188

Stickland, D. J. & Lloyd, C. 1993, The Observatory, 113, 256

Stickland, D. J. & Lloyd, C. 2001, The Observatory, 121, 1

Thackeray, A. D. & Andrews, P. J. 1974, A&AS, 16, 323

Vacca, W. D., Garmany, C. D., & Shull, J. M. 1996, ApJ, 460, 914

Vansina, F. & de Greve, J. P. 1982, Ap&SS, 87, 377

Vink, J. S., de Koter, A., & Lamers, H. J. G. L. M. 2000, A&A, 362, 295

ten Brummelaar, T., Mason, B. D., McAlister, H. A., Roberts, L. C., Turner, N. H., Hartkopf, W. I., & Bagnuolo, W. G. 2000, AJ, 119, 2403

Walborn, N. R. 1971a, ApJ, 167, L31

Walborn, N. R. 1972, AJ, 77, 312

Walborn, N. R. 1973, AJ, 78, 1067

Walborn, N. R. 1976, ApJ, 205, 419

Walborn, N. R. 1982, ApJ, 254, L15

Walborn, N. R., Nichols-Bohlin, J., & Panek, R. J. 1985, International Ultraviolet Explorer Atlas of O-Type Spectra from 1200 to 1900 Å, NASA RP-1155 (Washington: NASA)

Walborn, N. R., & Nichols-Bohlin, J. 1987, PASP, 99, 40

Walborn, N. R., & Panek, R. J. 1984, ApJ, 286, 718

Walborn, N. R. & Bohlin, R. C. 1996, PASP, 108, 477

Walborn, N. R., & Howarth, I. D., 2000, PASP, 112, 1446

Walborn, N. R., Howarth, I. D., Lennon, D. J., Massey, P., et al. 2002a, AJ, 123, 2754

Walborn, N.R., Fullerton, A.W., Crowther, P.A., Bianchi, L., Hutchings, J.B., Pellerin, A., Sonneborn, G., Willis, A.J., 2002b, ApJS, 141, 443

Walker, M. F. 1961, ApJ, 133, 438

Wamsteker, W., Skillen, I., Ponz, J. D., de la Fuente, A., Barylak, M., & Yurrita, I. 2000, Ap&SS, 273, 155

Table 1. Datasets used in this work

Star	*FUSE*	*IUE*	*HST-STIS*	*ORFEUS*
HD 190429A	P1028401	SWP38994		
HD 64568	P1221103	SWP29337		
HD 93250	P1023801	SWP22106		
HD 93205	P1023601	SWP14747	O4QX01010	
HDE 303308	P1221602	SWP07024	O4QX04010	
HD 96715	P1024301	SWP43980,SWP21999		tues5233_4
HD 168076	P1162201	SWP28277		

Table 2. The program stars

Star	Sp. Type [a]	Sp. Type Ref.	V	$B-V$	E($B-V$) [b]	log N_{HI} [c] $[cm^{-2}]$	log N_{H_2} [d] $[cm^{-2}]$	Distance (Kpc) [Kpc]
HD 190429A	**O4 If$^+$**; O4 f; O4 I O5 If+O9.5 III+B1 IIIs O4f+O9.5III ; O4If$^+$+O9.5 II O5f+B0III ; O5f+O9.5Ibp	(1,2,3;4;5) (8) (9,10;11) (12;13)	7.07(6)	0.09 (6)	0.41	21.29	20.31	2.3 (7)
HD 64568	**O3 V((f*))**; O4 V ((f)); O5 V O5; O5/6	(14,1;15;16) (19,20,21,22;23)	9.39 (17)	0.11 (17)	0.44	21.32	20.34	5.5 (18)
HD 93250	**O3.5 V((f$^+$))**; O3 V((f)); O3:V((f)); O3 V(f) O3 I; O3 III(f);O3 ; O5	(1;2,14,21,24;25;26) (5;29;4;13)	7.37(27)	0.17(27)	0.50	21.38	19.92/19.94[e] (28)	2.5 (25)
HD 93205	**O3.5 V((f$^+$))**; O3 V; O3 O3 V+O8 V	(1;14,21,2,25,24,26;4) (32,33)	7.75 (30)	0.05 (30)	0.38	21.33 (31)	19.52	2.5 (25)
HDE 303308	**O4 V((f$^+$))**;O4 V((f)) O3 V; O3 V((f)); O3 V(f);O3	(1;29) (24,2;3,14,21,25;26;4)	8.15(27)	0.12(27)	0.45	21.45 (31)	19.99/19.81[e] (28)	2.5 (25)
HD 96715	**O4 V((f))**; O4 V; O5:	(3,21;2,15; 26)	8.27 (34)	0.10 (34)	0.43	21.31	20.33	2.9 (3)
HD 168076	**O4 V((f))**; O4 V((f$^+$)); O5 V((f*)) O4 ((f)); O4f ;O5 ; O4 III(f)	(3;35;36) (10,4;9;13,23;29)	8.18 (36)	0.43 (36)	0.75 (36)	19.67/21.65[f] (37)	20.32/20.43[f] (37)	2.0 (36)

[a]Adopted types in bold face; other values from the literature are compiled. For multiple systems we also list here the spectral type of the companion (if known).

[b]If no reference provided, calculated from $B-V$ (this table) and $(B-V)_0$ (from Massey (1998)).

[c]If no reference provided, N_{HI} is derived from the relation of Bohlin, Savage, & Drake (1978), using E($B-V$) from this table.

[d]If no reference provided, $N_{H_2} = 0.5(N_H - N_{HI})$ and $N_H/E(B-V) = 5.8 \cdot 10^{21}\ atoms\ cm^{-2} mag^{-1}$ (Bohlin, Savage, & Drake 1978), using N_{HI} and E($B-V$) from this table.

[e]Column densities of the foreground cloud (first value) and the Carina nebula (second value).

[f]Column densities of the traslucent component of the hydrogen cloud (first value) and of the diffuse component (second value).

References. — (1) Walborn et al. (2002a), (2) Walborn (1972), (3) Walborn (1973), (4) Conti & Frost (1977),(5) Penny et al. (1996), (6) ten Brummelaar et al. (2000), (7) Morgan, Whitford, & Code (1953), (8) Abt (1986), (9) Conti & Alschuler (1971), (10) Conti & Leep (1974), (11) Walborn & Howarth (2000), (12) Guetter (1968), (13) Morgan et al. (1955), (14) Walborn (1982), (15) Garrison et al. (1977), (16) Peton-Jonas (1981), (17) Havlen (1972), (18) Kaltcheva & Hilditch (2000), (19) MacConnel & Bidelman (1976), (20) Crampton (1971), (21) Cruz-Gonzalez et al. (1974), (22) Lodén (1965), (23) Houk & Smith-Moore (1988), (24) Walborn (1971a), (25) Levato & Malaroda (1982), (26) Thackeray & Andrews (1974), (27) Feinstein (1982), (28) Lee et al. (2000), (29) Mathys (1988), (30) Feinstein, Marraco, & Muzzio (1973), (31) Diplas & Savage (1994), (32) Conti & Walborn (1976), (33) Morrell et al. (2001), (34) Schild et al. (1983), (35) Bosch, Morrell, & Niemelä (1999), (36) Hillenbrand et al. (1993), (37) Rachford et al. (2002)

Table 3. Stellar parameters from model fitting of Far-UV and UV spectra.

Star	Sp type	$T_{\rm eff}$ [kK]	log g	R/R$_\odot$	M/M$_\odot$	log(L$_{bol}$/L$_\odot$)	v_∞ [km s^{-1}]	$\dot{M}^{\rm a}$ [M$_\odot$ yr^{-1}]	$\dot{M}^{\rm b}$ [M$_\odot$ yr^{-1}]	$L_{\rm x}/L_{\rm bol}$
HD 190429A	O4 If$^+$	37.5±1.5	3.4±.1	25±2	57	6.05±.15	2100±200	$1.2\pm.2 \cdot 10^{-5}$	$9.2 \cdot 10^{-6}$	-6.5±.5
HD 64568	O3 V((f*))	41±2	3.9±.2	14±2	57	5.7±.2	2800±200	$5.6\pm5. \cdot 10^{-7}$	$2.3 \cdot 10^{-6}$	-7.5±.75
HD 93250	O3.5 V((f$^+$))	40±2	4.0±.2	12±2	53	5.5±.2	2900±200	$5.5\pm3. \cdot 10^{-7}$	$9.9 \cdot 10^{-7}$	-7.25±.25
HD 93205	O3.5 V((f$^+$))	40±2	4.0±.2	9±3	30	5.3±.2	3200±200	$3.3\pm2. \cdot 10^{-7}$	$5.1 \cdot 10^{-7}$	-7.0±.5
HDE 303308	O4 V((f$^+$))	40±2	4.0±.2	9±3	30	5.3±.2	2800±200	$3.4\pm2. \cdot 10^{-7}$	$6.0 \cdot 10^{-7}$	-7.0±.5
HD 96715	O4 V((f))	39±2	4.0±.2	9±3	30	5.2±.2	2800±200	$2.2\pm1. \cdot 10^{-7}$	$4.0 \cdot 10^{-7}$	-7.25±.25
HD 168076	O4 V((f))	39±2	4.0±.2	9±3	30	5.2±.2	2800±200	$2.2\pm1. \cdot 10^{-7}$	$4.0 \cdot 10^{-7}$	-7.0±.25

[a]This paper; values from spectral modeling

[b]Mass-loss rate value predicted with the mass-loss "recipe" of Vink, de Koter, & Lamers (2000), using the stellar parameters from our model fitting (this table)

Table 4. The parameters of the program stars previously derived in the literature

Star	$T_{\rm eff}$ [kK]	log g	log(L/$L_\odot$)	Ref.	R/$R_\odot$	M/$M_\odot$	Ref.	$\dot{M}$[a] [$M_\odot$ yr^{-1}]	v_∞ [km s^{-1}]	Ref.	$L_{\rm x}/L_{\rm bol}$	Ref.
HD 190429A	37.5	3.4	6.05	(1)	25	57	(1)	$1.2{\cdot}10^{-5}$	2100	(1)	-6.5	(1)
	28.2	3.53		(2)				$4.6\cdot10^{-6}$★ ; $< 2.1\cdot10^{-5}$★		(3;4)		
								$1.26\cdot10^{-5}$♦ ; $< 0.35\cdot10^{-6}$♣		(5;6)		
	33.1	3.00		(7)				$8.6\cdot10^{-6}$♦		(8)		
	47.5			(9)				$1.42\cdot10^{-5}$♦ ;$1.1\cdot10^{-5}$♦		(10;9)		
									1880	(11)		
HD 64568	41	3.9	5.7	(1)	14	57	(1)	$5.6{\cdot}10^{-7}$	2800	(1)	-7.5	(1)
											< -5.97	(12)
HD 93250	40	4.0	5.5	(1)	12	53	(1)	$5.5{\cdot}10^{-7}$	2900	(1)	-7.25	(1)
	37.2		5.75	(13)		46.5	(13)		3000	(14)	-6.4	(12)
	52.5	3.95	6.4	(15)	19	120	(15)	$1.3\cdot10{-}6$	3500	(16)		
	50.5	3.95/4.0[b]	6.28	(17)	18	118	(17)	$4.9\cdot10^{-6}$♦	3250	(17)		
	51.0	3.9	6.3	(18)		83.2/93.3/114.8[e]	(18)		3200;3230	(18;11)		
	46.0	3.95/3.96[b]	6.01	(19)	15.9	83.3	(19)	$3.45\cdot10^{-6}$ ♦		(19)		
	55.0			(9)				$4.1\cdot10^{-5}$★ ; $7.9\cdot10^{-8}$		(20;21)		
HD 93205	40	4.0	5.3	(1)	9	30	(1)	$3.3{\cdot}10^{-7}$	3200	(1)	-7.0	(1)
	55.0/36.5[c]			(22)	12.5/10.3 [c,f]	$\geq$39 / $\geq$15[c]	(22)	$> 5.9\cdot10^{-7}$	3600	(23)	-6.37	(23)
	44.7/35.5[c]		6.20/4.91[c]	(24)		100.00 / 24.82[c]	(24)					
	36.3		6.02	(13)		63.4	(13)					
			5.51/4.80[c]	(25)	8.0/6.3[c]	45/20[c]	(25)				-6.45	(12)
	55.0			(9)		$\geq$31.5 / $\geq$13.3[c]	(26)				$\sim$-7.0	(26)
						$\geq$37/$\geq$15[c]	(27)					
						$\geq$32.6 / $\geq$14.2[c]	(28)					
						63.3 / 24.5[c] ; $\leq$60/$\leq$25[c]	(29;30)					
HDE 303308	40	4.0	5.3	(1)	9	30	(1)	$3.4{\cdot}10^{-7}$	2800	(1)	-7.0	(1)
	48.0	4.05/4.10[b]	5.84	(17)	12	66	(17)	$2.1\cdot10^{-6}$♦	3100	(17)	-6.54	(12)
	45.5	3.9	5.8	(31)	13	50/60/70[d]	(31)	$2.5\cdot10^{-6}$	3400	(16)		
	35.5		5.27	(13)		28.8	(13)		3035	(11)		
	48.0	3.9	5.85	(18)		40.7/41.7/40.7[e]	(18)		3200;3000	(18;14)		
	41.0	3.90/3.91[b]	5.53	(19)	11.5	39.0	(19)	$1.63\cdot10{-}6$♦		(19)		
	55.0			(9)								
HD 96715	39	4.0	5.2	(1)	9	30	(1)	$2.2{\cdot}10^{-7}$	2800	(1)	-7.25	(1)
									2900;3000	(14;11)	< -5.85	(12)
HD 168076	39	4.0	5.2	(1)	9	30	(1)	$2.2{\cdot}10^{-7}$	2800	(1)	-7.0	(1)
	55.0	4.3		(32)				$2.51\cdot10^{-6}$♦		(5)		
	50.0			(9)				$1\cdot10^{-5}$♦		(9)		
									3305	(11)		

[a]Mass-loss rate calculated from line fit to IUE lines unless a different method is indicated with one of the following symbols: ★ analysis of radio data, ♦ analysis of Hα, ♣ analysis of IR data.

[b]log g derived from the fit to Hγ / Same but corrected for centrifugal force.

[c]Main component / Secondary component.

[d]M/$M_\odot$ calculated from: log g and radius / comparison with evolutionary tracks of high mass loss rate / same with tracks of low mass-loss rate.

[e]M/$M_\odot$ calculated from: v_∞vs M_*relation / log g and radius / comparison with evolutionary tracks.

[f] Assuming a distance of 2.6 Kpc to Tr16.

References. — (1) This work, (2) Salukvadze & Javakhishvili (1995), (3) Scuderi et al. (1998), (4) Abbott, Bieging, Churchwell, & Cassinelli (1980), (5) Leitherer (1988), (6) Persi, Ferrari-Toniolo, & Grasdalen (1983), (7) Oke (1954), (8) Scuderi et al. (1992), (9) Conti & Frost (1977), (10) Markova et al. (2004), (11) Howarth, Siebert, Hussain, & Prinja (1997), (12) Chlebowski et al. (1989), (13) Kaltcheva & Georgiev (1993), (14) Lamers, Snow, & Lindholm (1995), (15) Kudritzki (1980), (16) Garmany et al. (1981), (17) Puls et al. (1996), (18) Kudritzki et al. (1992), (19) Repolust et al. (2003), (20) Leitherer, Chapman, & Koribalski (1995), (21) Conti & Garmany (1980), (22) Conti & Walborn (1976), (23) Chlebowski & Garmany (1991), (24) Vansina & de Greve (1982), (25) Antokhina et al. (2000), (26) Morrell et al. (2001), (27) Corti, Albacete, Morrell, & Niemela (1999), (28) Stickland & Lloyd (1993), (29) Doom & de Loore (1984), (30) Benvenuto et al. (2002), (31) Simon et al. (1983), (32) Morrison (1975)

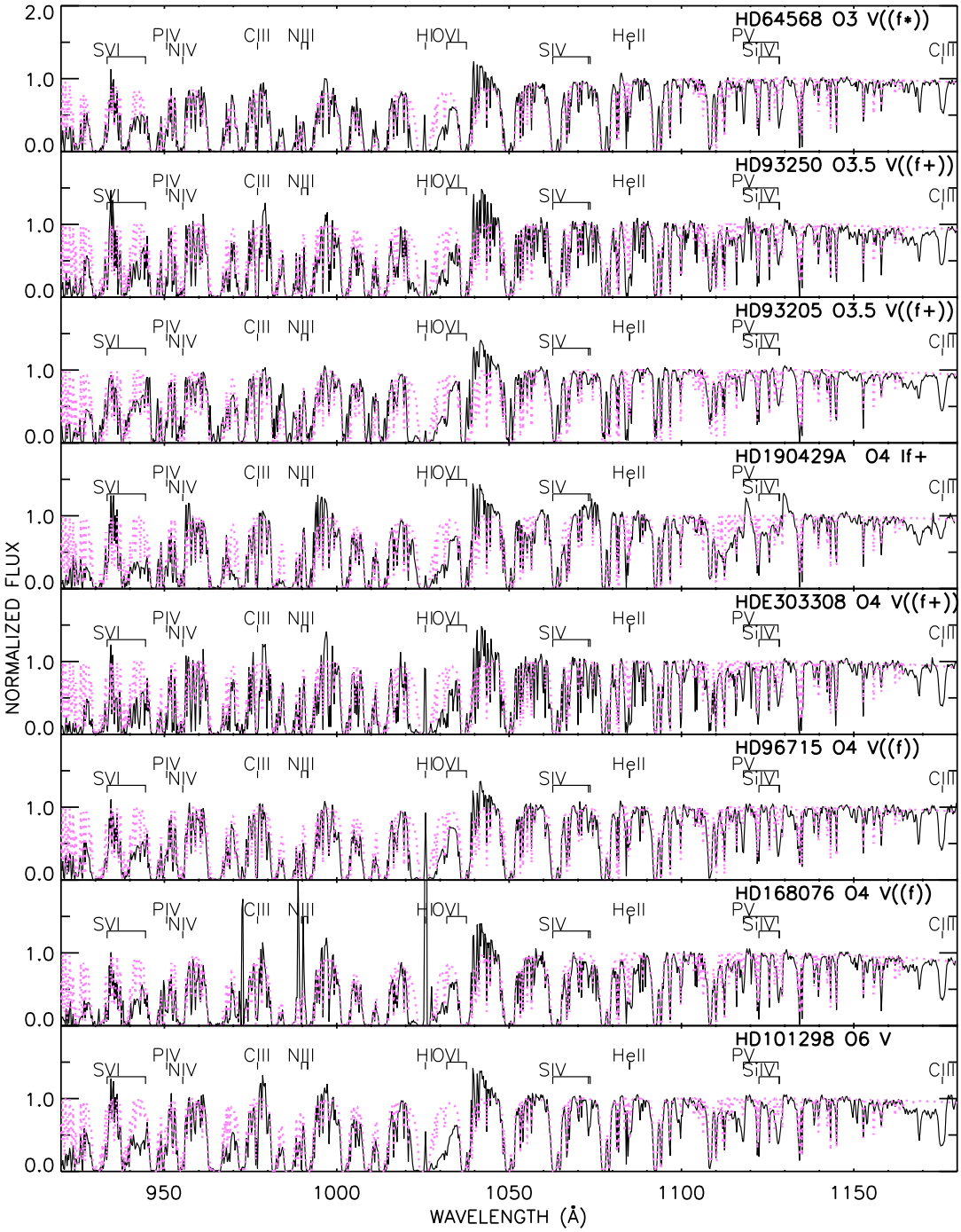

Fig. 1.— *FUSE* spectra of the O3-O4 type stars analysed in this paper and HD 101298 (O6 V, analysed in paper I), arranged by spectral type. The spectra are rebinned to steps of 0.25Å for clarity and normalized to the local continuum. The dotted (pink/light-grey) lines are interstellar hydrogen ($H_2 + HI$) absorption models, calculated for the line of sight of each star (see Section 2), that aid us to identify the genuine stellar features against the interstellar ones. Note the stronger profiles that P V $\lambda\lambda$1118.0,1128.0+Si IV $\lambda\lambda$1122.5,1128.3,1128.4 and C IV λ1169+C III λ1176 exhibit in the spectrum of the supergiant star. The dwarf stars have very similar spectral features, but there is a smooth increase of C III λ1176 and P V $\lambda\lambda$1118.0,1128.0+Si IV $\lambda\lambda$1122.5,1128.3,1128.4 from O3 V to O6 V.

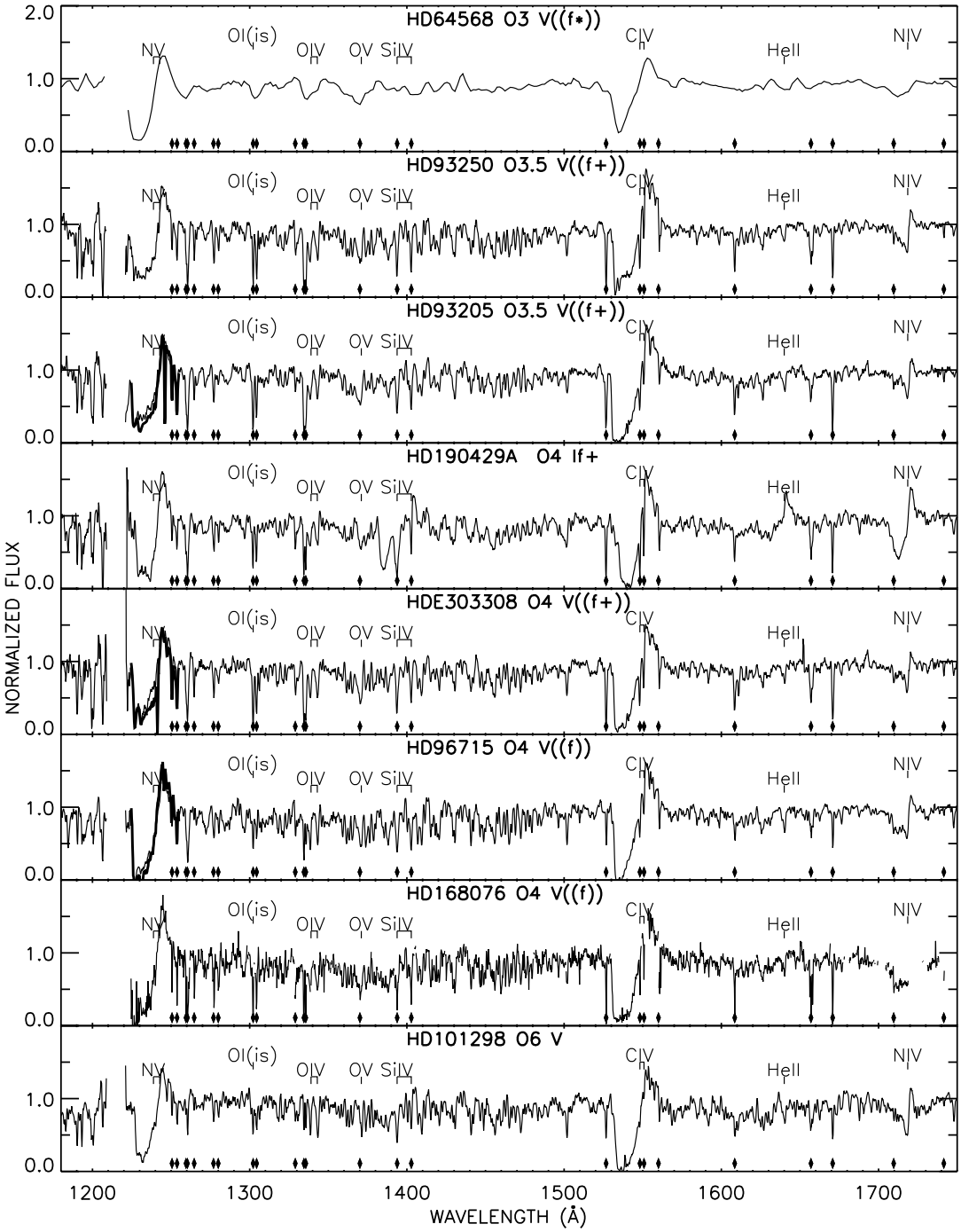

Fig. 2.— Normalized *IUE* spectra of the stars included in Figure 1. The spectra are rebinned to 0.25Å, except for the spectrum of HD 64568, which has low resolution (6Å). The positions of the most important interstellar lines are marked with diamonds at the bottom of the spectra. The *IUE* data have very poor quality in the Lyα region, which has been removed for clarity. The saturated portions have been removed from the spectrum of HD 168076. The thick lines plotted over the spectra in the N V $\lambda\lambda$1238.8,1242.8 region are *ORFEUS-TUES* data for HD 96715 and *HST-STIS* data for HDE 303308 and HD 93205. Note that the Si IV $\lambda\lambda$1393.8,1402.8 absorption weakens towards earlier spectral types. N IV $\lambda\lambda$1718.0,1718.5 and O V λ1371.0 and to a lesser extent, C IV $\lambda\lambda$1548.2,1550.8, increase from the O6 V to the O3.5 V stars. The most important luminosity effects are the stronger He II λ1640.0, Si IV $\lambda\lambda$1393.8,1402.8 and N IV $\lambda\lambda$1718.0,1718.5 P Cygni profiles of the supergiant spectra.

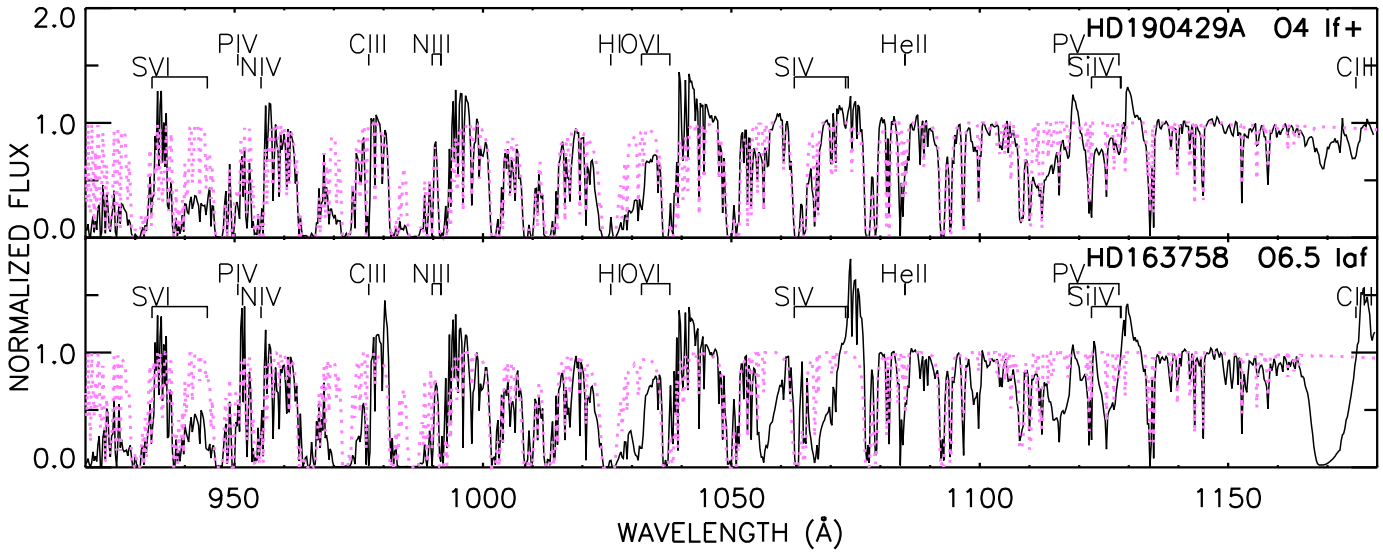

Fig. 3.— Temperature effects in luminosity class I: *FUSE* spectra of the supergiant stars HD 190429A (O4 If$^+$) and HD 163758 (O6.5 Iaf, from paper I) (colors/lines as in Figure 1). The strength of S IV $\lambda\lambda$1062.7,1073.0,1073.5 and C IV λ1169+C IIIλ1176 severely decreases towards higher $T_{\rm eff}$. Note also that the wind profile of the P V $\lambda\lambda$1118.0,1128.0+ Si IV $\lambda\lambda$1122.5,1128.3,1128.4 blend changes in shape, whereas the O VI $\lambda\lambda$1031.9,1037.6 P Cygni profile is almost identical in both spectra.

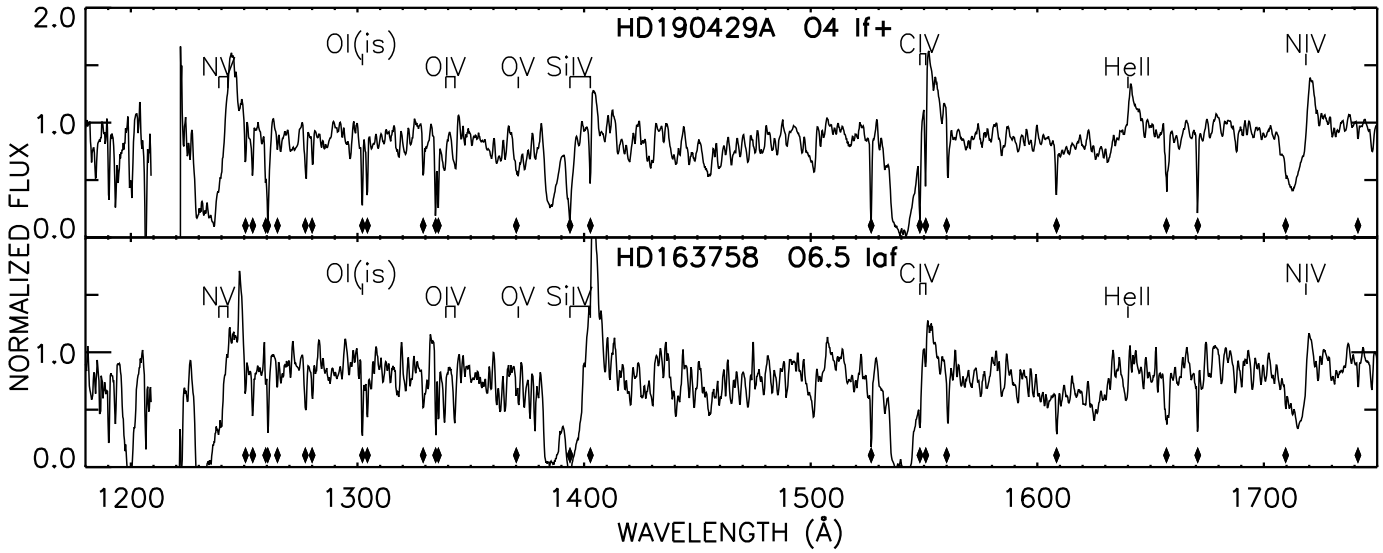

Fig. 4.— *IUE* spectra of HD 190429A and HD 163758 (lines/symbols as in Figure 2). The most outstanding differences are seen in the Si IV $\lambda\lambda$1393.8,1402.8 doublet and the He II λ1640.0 line. N IV $\lambda\lambda$1718.0,1718.5 and the emission of C IV $\lambda\lambda$1548.2,1550.8 are stronger in the earlier type star.

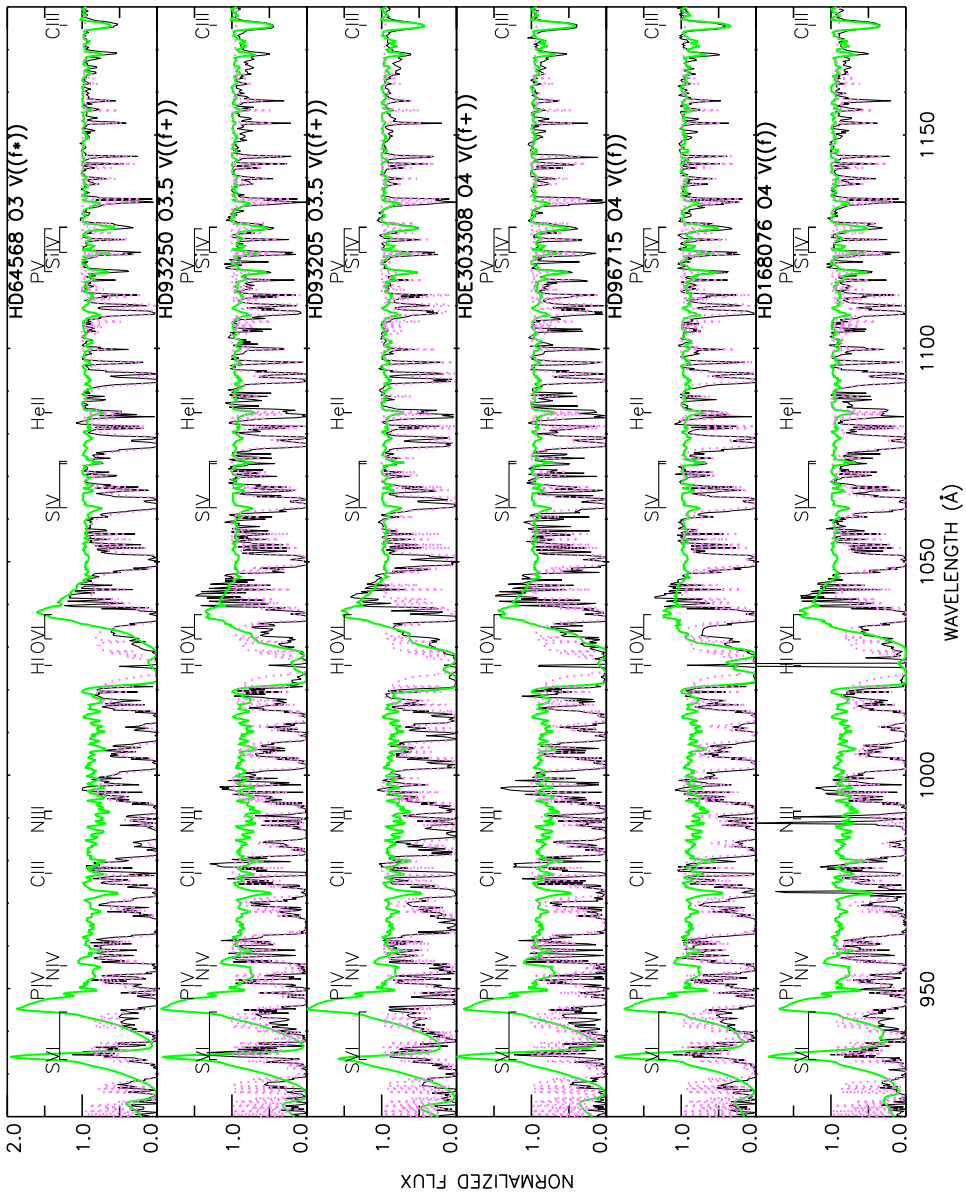

Fig. 5.— Best fit *WM-basic* models (green/grey) and *FUSE* spectra (black) of the dwarf stars of the sample. Models and spectra have been rebinned to 0.25Å steps. The dotted (pink/light-grey) line is the interestellar $H_2 + HI$ absorption model in the line of sight of each star. The $T_{\rm eff}$ of the models increases from 39,000 K (HD 160876, HD96715) to 40,000 K (HDE 303308, HD 93205 and HD 93250) and to 41,000 K (HD 64568). Note the good fit to C III λ1176 and P V $\lambda\lambda$1118.0,1128.0+ Si IV $\lambda\lambda$1122.5,1128.3,1128.4, the best indicators of temperature in this spectral range.

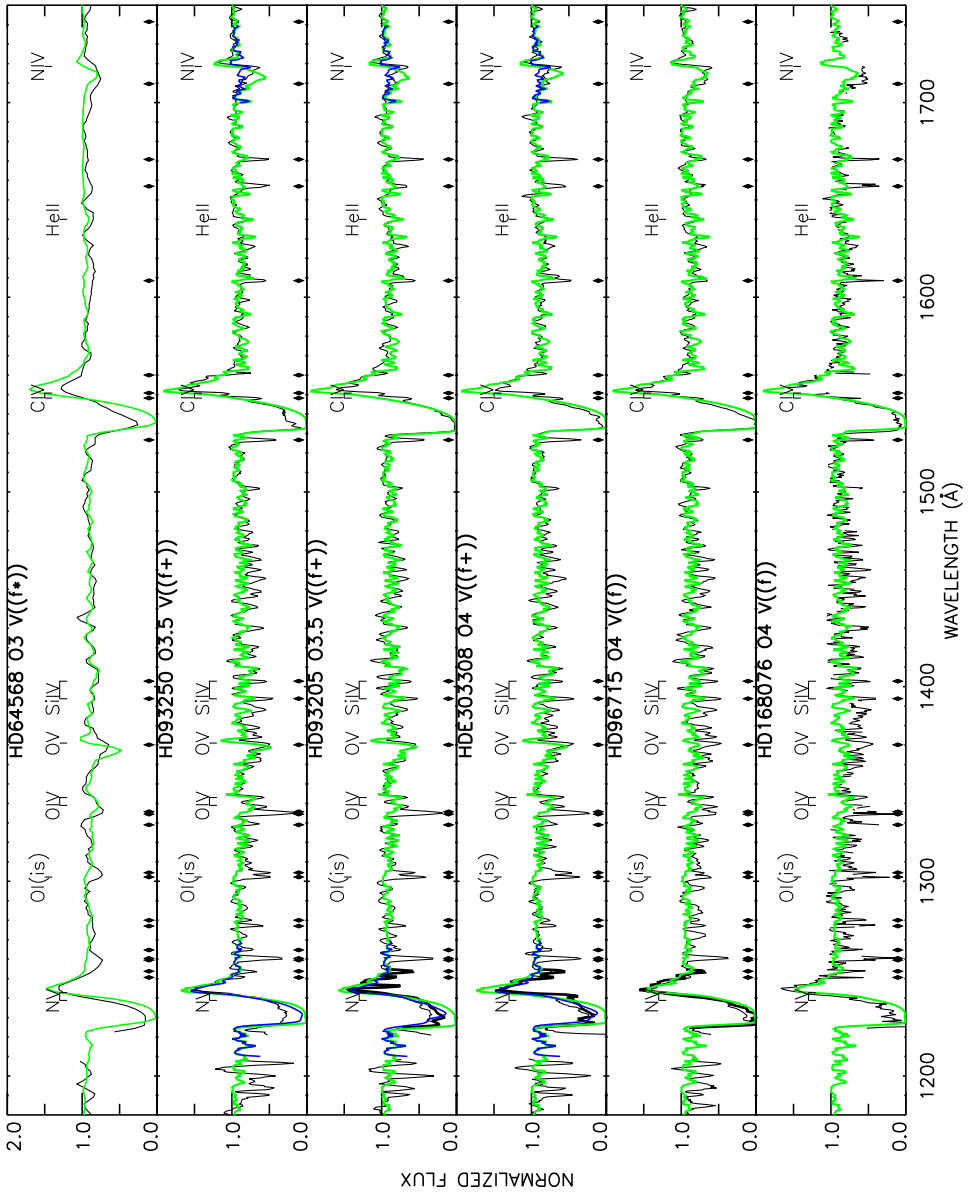

Fig. 6.— Same as Figure 5, IUE range. For HD 93250, HD 93205 and HDE 303308 we also include in blue/dark-grey the best fit model with an underabundance of nitrogen ($\epsilon_N = 0.1\ \epsilon_{N,\odot}$) in the spectral regions around N V $\lambda\lambda$1238.8,1242.8 and N IV $\lambda\lambda$1718.0,1718.5 (the rest of the model is identical to that with solar abundances). The observed and synthetic spectra have been rebinned to 0.5Å steps, except for HD 64568 (model rebinned to 6Å). Other lines and symbols have the same meaning as in Figure 2. The best $T_{\rm eff}$ indicators in this range are N IV $\lambda\lambda$1718.0,1718.5 and O V λ1371.0, which we successfully fit for all stars but HD 168076. The unsaturated N V $\lambda\lambda$1238.8,1242.8 profiles are discussed in the text. The model fits well the *ORFEUS* spectrum of HD 96715.

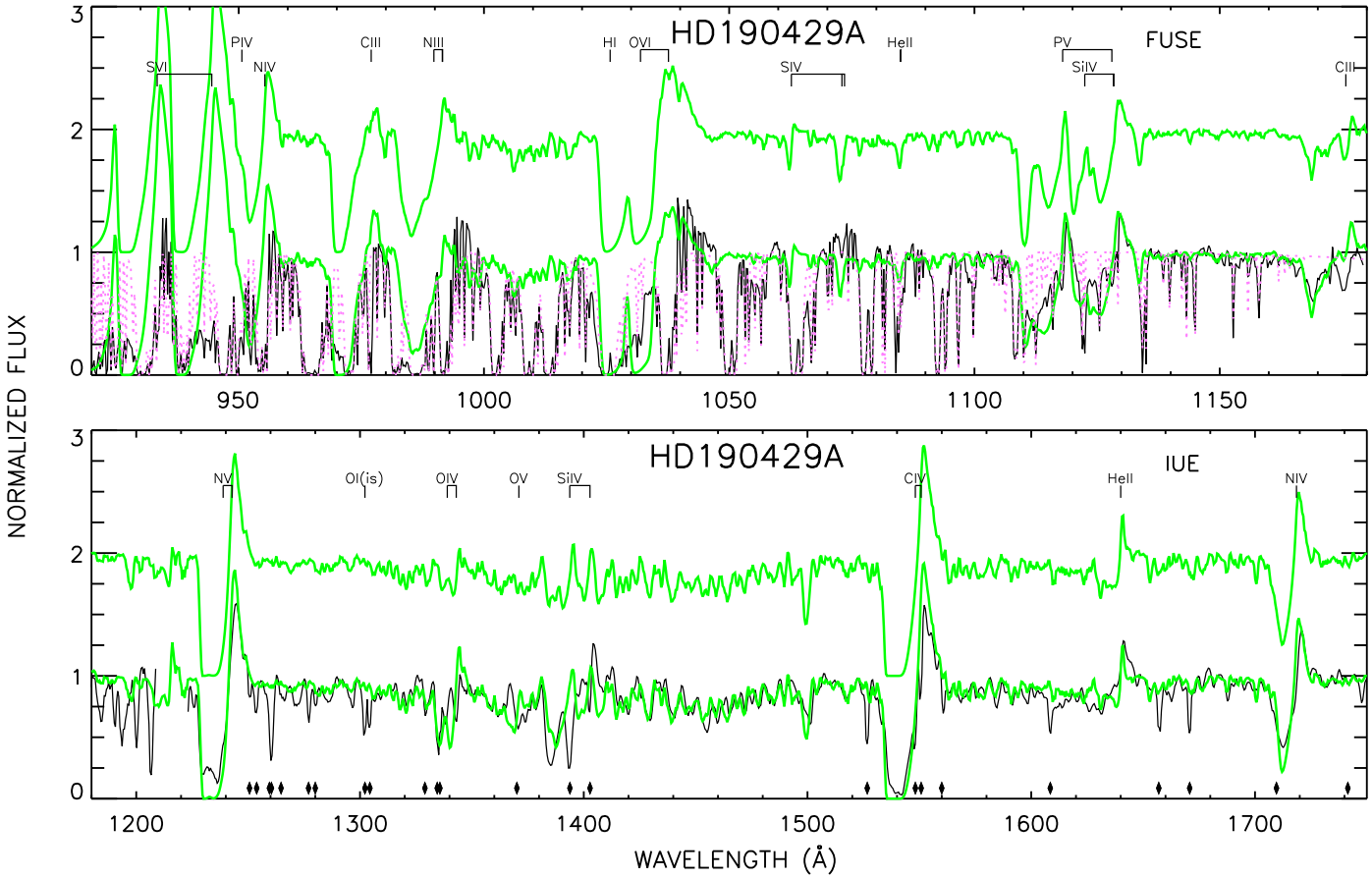

Fig. 7.— Best fit models of HD 190429A (top: *FUSE* spectra, bottom: *IUE* spectra). Two models (green/grey) are shown, both with $T_{\rm eff}$=37,500 K, log = 3.4, R= $25R_{\odot}$, $\dot{M}$= $1.2 \cdot 10^{-5}$ $M_{\odot}$ yr^{-1}, log$L_{\rm x}/L_{\rm bol}$ = -6.5 , $L_{\rm bol}$=6.05 and v_{∞}= 2100 km s^{-1}. The model superimposed to the spectrum, with solar abundances, provides a good fit of most wind features in both *FUSE* and *IUE* range. The top model has modified CNO abundances ($\epsilon_{He} = 5\ \epsilon_{He,\odot}$, $\epsilon_C = 0.5\ \epsilon_{C,\odot}$, $\epsilon_N = 2.0\ \epsilon_{N,\odot}$, $\epsilon_O = 0.1\ \epsilon_{O,\odot}$) and fits better C IV λ1169+C III λ1176 and O VI $\lambda\lambda$1031.9,1037.6, but less well P V $\lambda\lambda$1118.0,1128.0 and Si IV $\lambda\lambda$1393.8,1402.8.

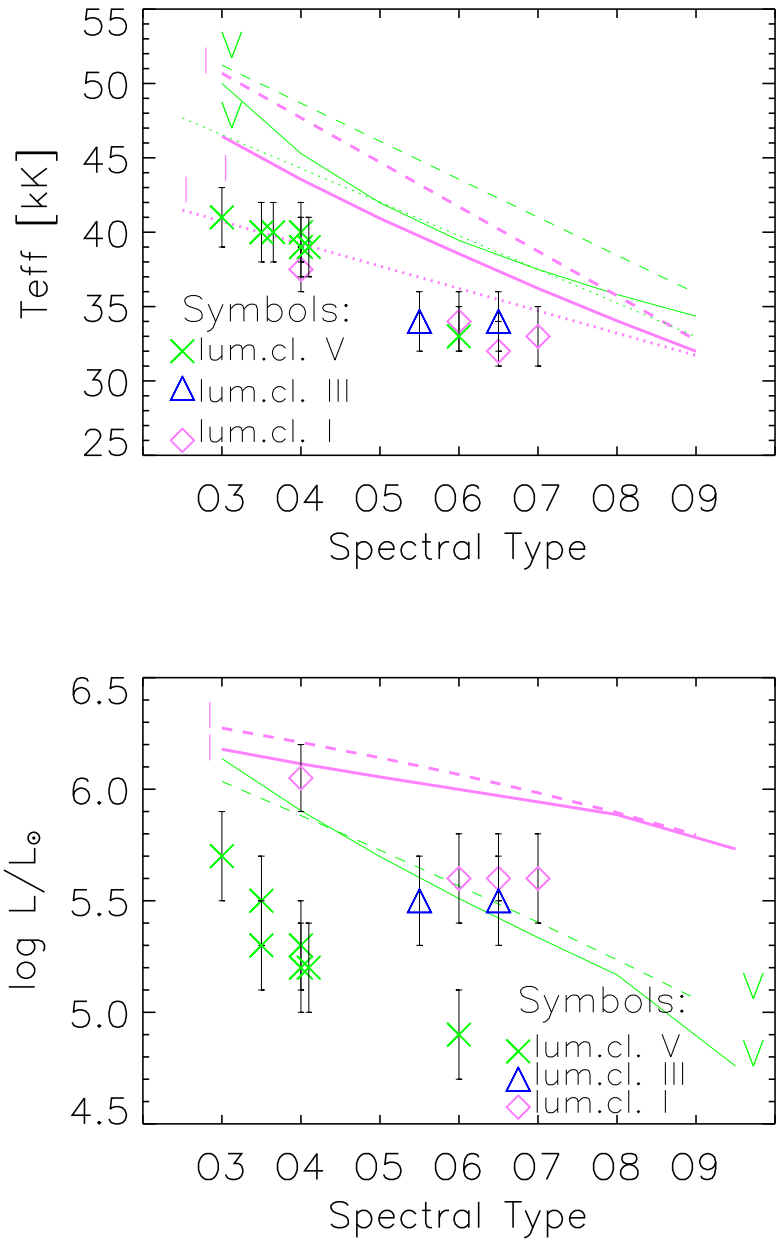

Fig. 8.— $T_{\rm eff}$ (top plot) and $L_{\rm bol}$ (bottom plot) obtained for the objects analysed in this paper and in Bianchi & Garcia (2002) are compared to the empirical calibrations of Vacca et al. (1996) (dashed line), de Jager & Nieuwenhuijzen (1987) (solid line) and Markova et al. (2004) (dotted line). The thick lines represent the curves for supergiants and the thin lines represent dwarf stars; the symbols for individual objects indicate luminosity class and are explained in the figures. Our temperatures and luminosities are lower than these previous calibrations.

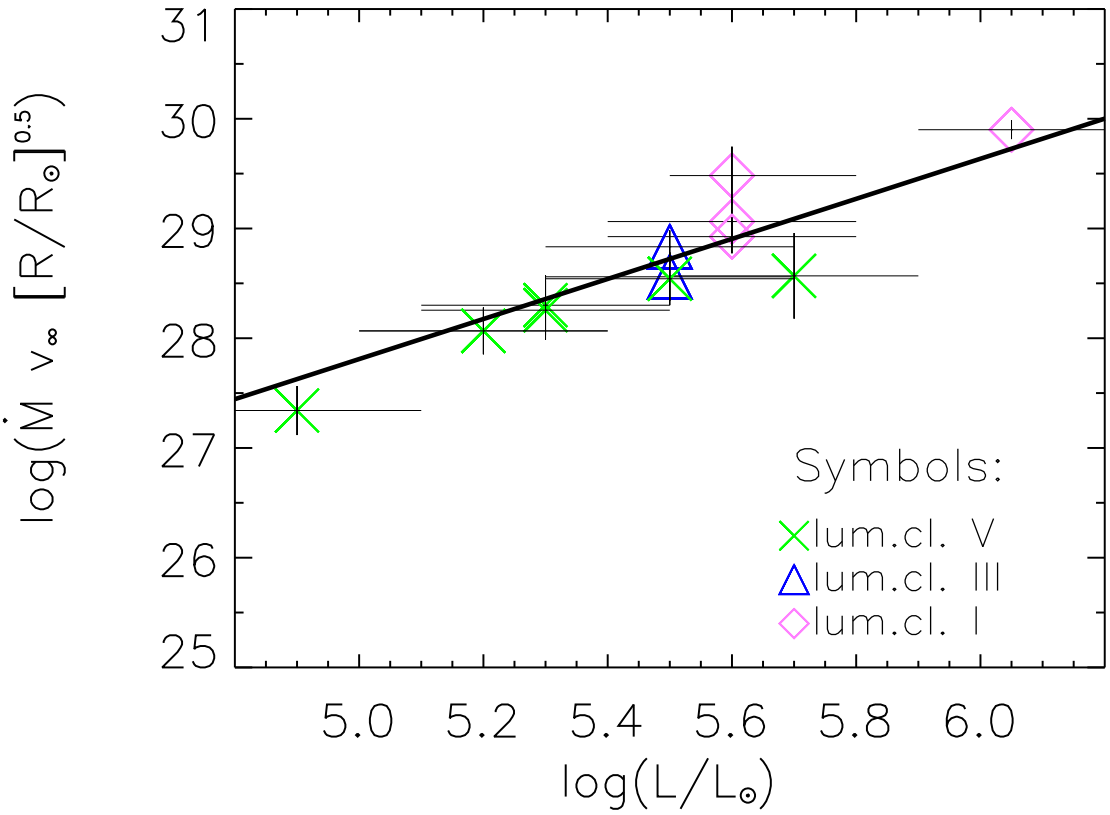

Fig. 9.— Modified wind-momentum *versus* luminosity for the objects of the present sample plus those analysed in paper I. The product $\dot{M}\cdot v_\infty$ is in cgs-units. Symbols represent individual objects of different luminosity classes and are explained in the plot. The solid line represents the theoretical WLR of Vink, de Koter, & Lamers (2000).